UNITED STATES DEPARTMENT OF THE INTERIOR

GEOLOGICAL SURVEY

Electrical Structure of Newberry Volcano, Oregon

by

D. V. Fitterman, W. D. Stanley, and R. J. Bisdorf

Open-File Report 88-245

1988

Abstract

From the interpretation of magnetotelluric, transient electromagnetic, and Schlumberger resistivity soundings the electrical structure of Newberry Volcano in central Oregon is found to consist of four units. From the surface downward the geoelectrical units are: 1) very resistive, young, unaltered volcanic rock, 2) a conductive layer of older volcanic material composed of altered tuffs, 3) a thick resistive layer thought to be in part intrusive rocks, and 4) a lower-crustal conductor. This model is similar to the regional geoelectrical structure found throughout the Cascade Range. Inside the caldera, the conductive second layer corresponds to the steep temperature gradient and alteration minerals observed in the USGS Newberry 2 test hole. Drill hole information on the south and north flanks of the volcano (test holes GEO N-1 and GEO N-3 respectively) indicates that outside the caldera the conductor is due to alteration minerals (primarily smectite) and not high-temperature pore fluids. On the flanks of Newberry the conductor is generally deeper than inside the caldera, and it deepens with distance from the summit. A notable exception to this pattern is just west of the caldera rim where the conductive zone is shallower than at other flank locations. The volcano sits atop a rise in the resistive layer, interpreted to be due to intrusive rocks. The intrusive material has served as a heat source to produce enhanced hydrothermal alteration, and, perhaps in the case of the west-flank anomaly, elevated fluid temperatures. While no public drill hole information is available to confirm this hypothesis, the west-flank anomaly appears to be a good geothermal target. In addition to the possibility that a region on the west side of the volcano could be favorable for prospecting, part of the resistive structure under the center of the volcano could be due to a vapor-dominated environment with temperatures above 300°C. In other parts of the Cascades pervasive alteration has produced mixed-layer clays and zeolites resulting in low-resistivity anomalies. Low resistivities can not be assumed to indicate high-temperature pore fluids. The use of electrical methods that measure resistivity as a function of excitation frequency, such as spectral induced polarization, may provide a way of obtaining information about the type and extent of alteration.

Introduction

Temperature strongly influences the physical properties of geologic materials. The electrical resistivity of fluid-saturated rocks, for example, decreases with increasing temperature up to temperatures of about 250°C [Parkhomenko, 1967; Olhoeft, 1981]. Because of this fact, electrical geophysical techniques have been used to explore for geothermal systems and to provide information about geothermal reservoirs. Temperature, however, is not the only factor that contributes to the resistivity of geologic materials; porosity, fractures, confining pressure, pore fluid chemistry, and mineralization within the pores also affect the resistivity. As a result, electrical geophysical techniques must be used carefully for geothermal exploration.

In order to assess the usefulness of electrical geophysical techniques for geothermal exploration in the Cascade Range, a suite of electrical geophysical methods have been used at Newberry Volcano, in central Oregon (see Figure 1). Newberry Volcano has been the subject of extensive research and exploration including geological, geochemical, and geophysical studies by the U.S. Geological Survey, other government agencies, universities, and industry. Interest in Newberry as a geothermal target was stimulated by U.S. Geological Survey test hole results that encountered 265°C fluids at a depth of 932m [Sammel, 1981]. This and other non-proprietary drilling programs [Black et al., 1984; Swanberg and Combs; 1986, Swanberg et al., this volume] provided an opportunity to learn a great deal about the electrical structure of Newberry Volcano and allowed assessment of the utility of electrical methods for geothermal exploration in the Cascades.

In this paper we report the results of magnetotelluric, transient electromagnetic, and Schlumberger soundings. The interpretation of these data is compared with available drill hole data to determine the rock types associated with the various geoelectrical units. These data are used to produce an electrical model of Newberry Volcano which can serve as a guide for the use of electrical methods for geothermal exploration in the Cascades.

Geology

Newberry Volcano is a large Quaternary volcano located east of the main axis of the Cascade Range and is very similar to Medicine Lake volcano in northern California with both having summit craters, large volumes of basalt, and very

young (600-1550 year-old) silicic flows. Its geology has been described in detail by MacLeod et al. [1982]. Newberry lies at the western end of a sequence of rhyolitic rocks which become progressively younger from east to west [MacLeod et al., 1975]. Numerous cinder cones and fissure vents cover the flanks of the volcano [MacLeod and Sammel, 1982]. These vents have a north-northwest alignment on the northwest flank and a south-southwest trend on the southwest flank. The alignments appear to be extensions of the "Sisters" fault zone and Walker Rim fault zone respectively [MacLeod and Sherrod, this issue]. The summit is marked by a 6- to 8-km wide caldera which is thought to be the result of a collapse after massive tephra eruptions.

The volcano has had a complex history of eruptions and a wide range of volcanism ranging from basaltic to rhyolitic composition [MacLeod et al., 1981]. Extensive deposits of ash-flow and air-fall tuffs are found on the east and west flanks of the volcano. The oldest such deposit has been estimated to have an original volume of more than 40km^3 [MacLeod and Sammel, 1982]. Volcanic and sedimentary units containing tuffaceous flows and detritus are generally quite conductive because the tuffaceous materials are readily altered to layered clays and zeolites. The tuffs are quite pervasive and probably pre-Newberry in age.

Electrical Sounding Techniques

Three different electrical methods were used to characterize the electrical structure of the volcano including magnetotelluric (MT) [Stanley, 1982], transient electromagnetic (TEM) [Fitterman, 1983; Fitterman and Neev, 1985; Fitterman et al., 1985], and Schlumberger resistivity (SR) soundings [Bisdorf, 1983 and 1985]. Figure 2 shows the location of all of the soundings. Also shown on the map are the locations of the U.S. Geological Survey's Newberry 2 test hole [Sammel, 1981] and the GEO Operator Inc.-Department of Energy cooperative holes GEO N-1 and GEO N-3 [Swanberg and Combs, 1986].

Magnetotelluric Soundings

MT soundings in the Newberry Volcano region have been employed as part of a regional study of the Cascades. The magnetotelluric (MT) method measures naturally occurring magnetic and electrical fields which are used to compute an apparent resistivity matrix as a function of frequency at the sounding site [Vozoff, 1972]. The data from this study were inverted to obtain 1-D interpretations which are pieced together to produce a cross section. Thirty five

MT soundings have been completed in the Newberry area at the locations shown in Figure 2. The MT survey was designed to map the gross structure of Newberry Volcano and its relationship to the rest of the Cascades. The soundings were concentrated on the west side of the volcano to study a shallow conductive zone detected by TEM [Fitterman and Neev, 1985] and SR soundings [Bisdorf, 1985].

The Newberry area presented considerable difficulty in completing the MT soundings. A thick covering of extremely high-resistivity pumice and sand composed of volcanic clasts caused problems with high contact impedance. Underground power lines in the central part of the caldera introduced noise at the locations where road access existed.

In general, the sounding data were approximately 1-D in nature as shown by the composite plot of the amplitude curves in Figure 3. Some exceptions to the 1-D character are shown in Figure 4. The main distortion of the soundings consists of parallel splitting of the two observed mode curves which is attributed to local, near-surface inhomogeneities [Berdichevsky and Dimetriev, 1976; Park, 1985]. The choice of mode for the 1-D interpretations was predicated on obtaining models that were both slowly varying laterally and were consistent with other data sets such as gravity.

The absence of a consistent polarization direction related to geologic structure allowed the independent rotation of the data at each frequency. In most instances the data are very insensitive to rotation angle, as is required by the 1-D assumption used in interpreting the data.

Examples of data from the western flank of the volcano are shown in Figure 3. The data were obtained from real-time processing of times series of 2048 points. Coherency sorting of the data using the multiple coherence function resulted in keeping only the best data with eight degrees of freedom. This was accomplished by using cascade decimation of a basic 128 point time series window. Thus, each 2048 point record was broken into 16 shorter time series for coherency sorting. As a result, nearly all of the data shown have multiple coherences of greater than 0.9. For most of the data on the western half of the study area were collected and processed with an MT system using two LSI-11/73* microcomputers (one with an array processor) that allowed real-time processing of the data. Two frequency bands were processed simultaneously; the array processor CPU was used for the

* The use of trade names is for descriptive purposes only and does not imply endorsement by the U.S. Geological Survey

0.1-2Hz and 1-12Hz bands, while the other CPU was dedicated to the 0.006-0.2Hz band. This allowed very efficient sounding execution. All six of the soundings shown (Figure 3) were completed in six hours, including setup and takedown of the equipment.

The MT sounding curves (Figure 3) are characterized by high resistivity at high frequencies, a minimum near 1Hz, a maximum near 0.05Hz, and a decrease in apparent resistivity with decreasing frequency at the end of the measurement range. This pattern is produced by a four-layer model with a conductive second and fourth layer. The data in this paper were interpreted with four or five-layer models using interactive forward and generalized inverse methods.

Transient Electromagnetic Soundings

The TEM soundings are made using a controlled-current source attached to a square transmitter loop about 300m on a side. The transmitter supplies a constant current to the loop which is periodically turned off and then turned on with opposite polarity. The current produces a primary magnetic field. When the transmitter current is rapidly turned off, the primary magnetic field collapses and a current system is induced in the ground below the transmitter loop. The diffusion of this current system in the ground is controlled by the conductivity structure below the transmitter site [Nabighian, 1979; Kaufman and Keller, 1983]. By measuring the decaying secondary magnetic field, information about the resistivity structure can be obtained. In practice, the voltage induced in a coil at the center of the transmitter loop by the time varying secondary magnetic field is recorded. The voltage data were converted to late-stage apparent resistivity [Kaufman and Keller, 1983; Fitterman and Stewart, 1986; Spies and Eggers, 1986] and were interpreted with layered models using the inversion scheme of Anderson [1982].

Figure 5 shows examples of TEM soundings from locations inside (3) and outside (5 and 37) the caldera. The data were interpreted with the minimum number of layers that gave a good fit. This typically results in a model with two or three layers. Because the high near-surface resistivities outside the caldera and the delay between the transmitter turnoff and the start of measurement of the transient (as much as 1.2ms), the first-layer resistivity is often not well determined. The first-layer resistivity was sometimes constrained during initial interpretation using VLF resistivity data measured along a profile traversing the TEM transmitter loop. The VLF apparent resistivities were usually greater than

1000Ωm. As the corresponding skin depths were over 100m, the apparent resistivities gave very good starting estimates for the first layer resistivity. Once a a reasonable resistivity model was determined, the first layer resistivity was allowed to vary during final inversion.

The resistivity models for the three soundings shown in Figure 5 are given in Figure 6. A characteristic of all the soundings, is that the resistivity decreases with depth. In general, the surface and bottom layers for the TEM models are more conductive inside (3) the caldera than on the flanks. Outside the caldera (5 and 37) the surface resistivity and depth to the conductor increase dramatically.

Schlumberger Resistivity Soundings

Schlumberger resistivity sounding is a direct-current electrical technique which uses a symmetric, collinear array of four electrodes to determine the electrical structure of the ground. Current is injected into the ground using the outer pair of electrodes while the electric field is measured between the inner pair of electrodes. By expanding the current electrode separation (AB/2) the depth of investigation is increased. The measured potential is converted to apparent resistivity and interpreted using layered-earth models [Zohdy, 1973, 1975].

Because of the sinuous nature of the roads in the field area, the standard technique used for Schlumberger soundings was modified. Instead of expanding the current bipole in a straight line, the current electrodes were expanded along the existing roads and the position of the current electrodes computed from topographic maps. A correction was then made before the data were interpreted for the actual AB/2 distance and the component of electric field measured [Zohdy and Bisdorf, 1982].

Figure 7 shows the apparent resistivity soundings curves and interpretations for soundings 1, 6, and 204. Sounding 1 is located inside the caldera, sounding 6 is on the western flank of the volcano, and sounding 204 is on the southern flank of the volcano (see Figure 2). The data show a pattern similar to that seen by the TEM and high-frequency MT data: In general, interpreted resistivity decreases with depth, and the most conductive material is located inside the caldera.

Comparison of the Techniques

The various electrical techniques used have different depths of investigation and sensitivities to conductive and resistive features. Therefore, a composite

geoelectrical model was developed using parts derived from all of the sounding techniques mentioned above.

The MT data sound deeper than the TEM and SR methods, providing information about features as deep as 20km and giving better estimates for the resistivity of the extensive conductor which underlies the volcano. However, because of an instrumental 12Hz upper frequency limit, the MT data do not give reliable resistivity estimates for the near surface material. In addition, the MT soundings are susceptible to severe problems due to near surface distortions of the electric field by surficial conductivity anomalies. This was not a major concern except inside the caldera as indicated by the sounding data shown in Figure 4. Our MT instrumentation has recently been modified to obtain data up to 400Hz. Such data would provide much better resolution of the near-surface layers. The MT data could be augmented with AMT soundings up to 20kHz using our current instrumentation.

The TEM method has high sensitivity to conductive zones that results in good vertical resolution. Of the three techniques used, the TEM method provides the best estimate of depth to a conductive target. A disadvantage is that the TEM data can not provide good resistivity estimates of high-resistivity zones such as the young, near-surface volcanic deposits found on the flanks of Newberry.

The SR data provide the best information about the shallow electrical structure. They give reliable resistivity information for high-resistivity zones, which is unobtainable from the MT and TEM data. However, the high near-surface resistivities encountered at Newberry (often in excess of 10kΩm) make it difficult to inject large currents thereby limiting the measurable signal and depth of investigation for the SR method.

All of the electrical data were interpreted assuming 1-D models. As discussed above, some of the MT data show the influence of non-1-D geometry. Due to the large arrays needed to sound deeply, the SR data may in some situations be influenced by lateral resistivity boundaries thereby introducing geologic noise into the layered-earth interpretations. The TEM data are minimally influenced by lateral inhomogeneities because the loop size is small compared to the measurement depth, and the measured signal is produced by current flowing on all sides of the receiver. Because our objective was the determination of the gross structure of the volcano and not small-scale features and because the effect of non-1-D geometry was small, we believe that our use of 1-D models is justified.

Regional Geoelectrical Structure

Several regional east-west MT profiles in the Cascades of California, Oregon, and Washington have been described by Stanley [1982 and 1983]. Most of the data from northern California and Oregon can be interpreted with a relatively simple four-layer model (Figure 8) with the following units, progressing from the surface downward:

1) a surface layer of Quaternary volcanic flows of 200Ωm to 2000Ωm resistivity that are 0.5km to 1.5km thick;

2) a variable layer consisting of probable Tertiary volcanic flows and/or Tertiary sedimentary rocks and volcanoclastics with resistivities of 5Ωm to 30Ωm and a thickness of 1km to 4km;

3) a 7km to 15km thick upper-crustal resistive zone with resistivities of greater than 100Ωm which represents the main part of the pre- and early-Tertiary accreted crust and Tertiary intrusives;

4) a lower-crustal conductor with resistivities of less than 10Ωm that occurs at depths of 8km to 20km which is believed to be related to partial melting and/or the presence of free water in the lower crust [Stanley, 1977; Wannamaker, 1986].

A structural trough in the resistive upper-crustal layer between the main axis of the Quaternary Cascade volcanoes and Newberry Volcano is observed on this and other east-west profiles in Oregon [Stanley, 1982]. The Newberry volcanic center appears to sit atop a significant structural high which is probably an igneous buildup into the Tertiary sedimentary/volcanic blanket that covers central Oregon.

Geoelectrical Structure of the Volcano

The electrical structure of Newberry Volcano consists of a resistive first layer and a conductive second layer that overlie a resistive basement forming a structural high beneath the volcano. All of these layers sit atop a lower-crustal conductor as detected by MT soundings.

Figure 9 shows the interpreted resistivity value at a depth of 250m based upon Schlumberger data. This depth was chosen to give a representative picture of the younger, near-surface volcanic units. The resistivities range from 65Ωm to 800Ωm inside the caldera with most of the values less than 200Ωm. (In this

section, we refer to the interpreted geoelectrical model parameters at the sounding sites. The contoured values may span a greater range inside and outside the caldera due to the inter-sounding spacing and data interpolation.) The resistivity of the surface layer increases towards the edges of the caldera. Outside the caldera the resistivities are generally in excess of 1000Ωm; at shallower depths, the resistivity can exceed 10kΩm in the first 50-100m.

The depth to the conductive second layer determined using TEM data is shown in Figure 10. Inside the caldera the depth ranges from 400m to 650m. Outside the caldera the depth to the conductive material increases, in general, with increasing distance from the caldera. A notable exception to this is found on the west flank where a region with depths of less than 500m is found. This shallow conductor is also seen in the MT and SR data.

The resistivity of the conductive second layer has been estimated using the TEM and MT sounding data. The TEM resistivities range from 2Ωm to 25Ωm inside the caldera (Figure 11). On the flanks the values increase from the intra-caldera values to 70Ωm. In the region to the west of the caldera, where the conductor is shallowest, its resistivity is generally 20Ωm to 25Ωm. A broad, low-resistivity region is present 7km south of Paulina Lake in the vicinity of the GEO N-1 test hole. In general the conductive second layer becomes less conductive at greater distances from the caldera.

The second-layer resistivity map interpreted from MT data (Figure 12) has a broad region of less than 10Ωm encompassing most of the caldera and extending to the west of the caldera. East of the caldera about 2km, there is a suggestion of a conductive region, however, the low station density does not define the region very well. Outside the caldera the conductor resistivity rises to greater than 25Ωm to the southwest. While the TEM coverage is more complete, the MT data provide better estimates of the resistivity because of its greater depth of exploration. The conductive second layer was also detected by the SR data, however, the interpreted resistivity values tend to be higher [Bisdorf, 1985]. The higher interpreted resistivities of the SR data may be due to anisotropy of the flows and is discussed below.

MT data provide the only information about the thickness of the conductive second layer. Figure 13 shows the estimated depth to the resistive third layer or electrical basement. In general the resistive basement becomes shallower towards the summit of the volcano, being 2km deep inside the caldera and ranging

from 1.5km to 4km deep outside. A noticeable, but poorly constrained, deviation from this trend is the shallow region west of the caldera.

The accuracy of our MT models is difficult to evaluate. The distortion due to near-surface inhomogeneities exhibited in the data from Figure 4 is difficult to treat. Many methods have been outlined to constrain the level of the two sounding curves including using independent measurements of ρ_1 [Stanley, 1980], computation of a distortion tensor based upon geomagnetic data [Larsen, 1975], determining a regional strike-local distortion tensor [Zhang et al., 1987], and constraining a particular resistivity in the section which is relatively constant [Jones, 1987]. We have utilized the latter method in dealing with the surface distortions of the data from inside the caldera. This method assumes that some layer thickness or resistivity is constant over the survey area, and the measured data are shifted to accommodate this constraint. In our situation we fixed the second layer resistivity at a value of 8Ωm for those data that were highly parallel shifted (evidence for near-surface distortion). The maximum error for this assumption in combination with normal measurement and least-squares fitting errors could be very large. However, confidence in the models is inspired by the good agreement between the TEM and MT interpretations for the top of the second layer. If the MT distortion-effect treatment had been severely in error, this would be reflected by major disagreements between the two methods.

The nature of the resistive structural high beneath Newberry is illustrated in the east-west section in Figure 14. The first layer resistivity was obtained from the SR data. The average longitudinal resistivity (total thickness divided by total conductance) was computed from the SR data from the surface down to the depth of the conductive second layer as determined by the TEM data. These values are substantially lower than the interpreted resistivities at a depth of 250m (see Figure 9) because the of the bias of the longituidinal averaging procedure in favor of conductive values. The first layer resistivity ranges from 250Ωm to 2900Ωm on the flanks of the volcano, with the eastern flank being more resistive. Inside the caldera the first layer is more conductive (80-180Ωm).

The top of the second layer as determined by the TEM and MT data is shown in the cross section. There is good agreement between the two methods with the greatest discrepancy on the eastern flank. These large discrepancies may be due to greater surface distortion effects on the MT data; a line of cinder cones passes through the eastern part of the survey area and may cause major inhomogeneities in the electric field. The closer spacing of the TEM data indicates a few more

features: the most notable being a rise in the conductive second layer just inside the caldera boundaries. A rise in the conductor top is also seen about 3km west of the caldera rim. The conductor resistivities as determined by the TEM data are generally higher than those determined by the MT data. In view of the greater depth of investigation of the MT method, this suggests that the second layer may become more conductive with depth.

Comparison of Geoelectrical Model and Drill Hole Data

Drill hole data provide an important key in explaining the geoelectrical data. Core samples reveal that fragmental flows and tuffs, and lacustrine sediments make up the first 500m of caldera material [MacLeod and Sammel, 1982], while young flows and tuffs which have very low water content are found at similar depths on the flanks of the volcano [Swanberg and Combs, 1986]. This accounts for the lower first-layer resistivity inside the caldera than outside.

The most interesting feature of the geoelectrical structure from a geothermal exploration view point is the conductive second layer. Possible explanations for the extensive conductor are that it is: 1) the water table, i.e., the boundary between dry and water saturated rocks, 2) rock saturated with high-temperature, conductive pore fluid, or 3) alteration minerals which have been deposited in the fractures and pore space of the rock.

The idea that the conductor is related to the water table is suggested by the location and geometry of the TEM conductor. The conductor elevation is about 1500m in the vicinity of the caldera, and drops to less than 1000m and 700m on the eastern and western flanks respectively. This surface is similar to the water table which would be expected as a result of meteoric water percolating downward through the volcanic material until it reaches the regional water table. Indeed, hydrologic studies suggest that some water may move laterally out of the caldera and through the flanks of the volcano [Sammel and Craig, 1983]. There are two factors, however, that argue against this explanation. First, analysis of ground water from shallow wells in the caldera indicates that resistivities are in the range of 20-100Ωm (specific conductivity of 100-600μmho/cm) [Sammel and Craig, 1983]. Assuming that temperatures on the flanks of the volcano in the first kilometer are not substantially different from surface conditions, it is unlikely that such resistive pore fluids could produce rock resistivities of less than 100Ωm. Second, the conductor lies below the regional water table by several hundred meters. Based on water well information, the regional water table is at

an elevation of 1310m (L. A. Chitwood, personal communication, 1985). The GEO Operator N-1 and N-3 holes confirm the level of the regional water table. At GEO N-1 and GEO N-3 the conductor is interpreted to be below the water table by almost 300m and 450m respectively. One would expect a better correlation between the conductor and water table elevations if pore fluid saturation were responsible for the conductor.

The second explanation, that the conductor is associated with high-temperature pore fluids, is suggested by the temperature log from the U.S.G.S. Newberry 2 test hole (Figure 15). The temperature log divides into three zones: the first (0-300m) having temperatures of less than 40°C, the second (300-675m) dominated by a convective zone with temperatures as great as 100°C, and the third (675-932m) characterized by a conductive thermal gradient. Sammel [1981] has pointed out that the temperature decreases at depths of 120m, 275m, 550m, and 625m are associated with rocks of high permeability carrying colder water. The interpreted TEM and SR data show a decrease in resistivity near 450m which corresponds to the temperature peak in the convective zone. Unlike the TEM and SR data, the MT data were interpreted with a constant resistivity to a depth of 1000m. Inside the caldera hot pore fluids at depth may, therefore, contribute to the low observed resistivities. With the exception of the resistivity increase near 950m in the SR data, there are no indications of a resistivity change associated with the high temperatures below 675m. The increase in the interpreted SR resistivity at depth could be caused by steam or by clogging and sealing of pore space by high-temperature alteration minerals. SR soundings inside the caldera and farther to the east did not detect a similar increase in interpreted resistivity at depth while those to the west of Newberry 2 did [Bisdorf, 1983] suggesting that lateral boundaries may also be a factor in producing the observed resistivity increase.

The interpreted resistivities for the soundings at the GEO Operator N-1 test hole (Figure 16), decrease with depth and are in good agreement with each other with the exception of the first layer for the MT sounding. The resistivity of the first layer was not well determined by the MT data. Furthermore, an attempt was made to use the lowest resistivity value permissible. The sounding data locate the top of the conductor between 735m and 900m. The agreement between the well logs and interpreted resistivities is good below a depth of about 600m. The low induction log resistivities between 150m and 475m are most likely caused by

disturbance of the rock due to invasion of mud and water during drilling and cleaning of the hole respectively.

The temperatures in the GEO N-1 hole at a depth of 1226m is only 74°C [Swanberg et al., this issue], significantly lower than the Newberry 2 bottom hole temperature. At a depth of 725m, the conductor depth based upon TEM measurements, the temperature is only 7.3°C and a large temperature gradient was not present. At Newberry 2, on the other hand, the temperature at the top of the conductor was high (100°C) and a gradient exists. North of the caldera at the GEO N-3 hole the conductor appears to be at a depth of between 760m and 980m based upon the three sets of sounding data (Figure 17). In this depth range the bore-hole temperature averages about 42°C [Swanberg et al., this issue]. The temperature log, however, does not show any significant gradients between 620m and 1160m due to artesian flow. Although temperature may contribute to the conductivity boundary it is not the principle cause.

The third explanation for the conductor is that it is a result of alteration minerals which line pores and fractures thereby lowering the bulk resistivity of the rock. In Figure 15 the occurrence of smectite alteration at Newberry 2 is indicated on the temperature-depth plots [Bargar and Keith, 1984; Keith et al., 1984]. Hydrothermal minerals are present at depths below 300m with a heavy concentration of smectite between 350m and 750m, the top of which is close to the conductor depth. A similar situation is seen at GEO N-1 (Figure 16) where the smectite alteration at a depth of 675m is in agreement with the top of the conductor [Bargar and Keith, 1986]. Wright and Nielson [1986] found that low-resistivity zones in the GEO N-1 induction log correspond to zones of basaltic ash and ash-flow tuff which have been altered to smectite. These zones while rather thin (1-3m) had resistivities ranging from 1.5-15Ωm suggesting that the presence of smectite throughout the section could produce the interpreted bulk resistivities of 8-30Ωm for the conductor. This is particularly true as TEM and MT measurements are sensitive to the high longitudinal conductance of thin conductive zones. While zeolite mineralization has been observed to produce low resistivities in volcanic rocks (G. R. Olhoeft, personal communication, 1986), these minerals are not present in the Newberry cores in as high concentrations as smectite (T. Keith, personal communication, 1986) possibly because they are not stable at higher temperatures. The zeolites probably do not contribute significantly to the overall conductivity, unless their meager occurrence very

efficiently covers all of the pore space with a thin coating, in which case they would have a significant effect.

At the Newberry 2, GEO N-1, and GEO N-3 holes the SR layer resistivities are higher than TEM values. This is partially due to anisotropy of the volcanic layers, and the fact that the sounding curves did not reach an asymptotic value. The layers are characterized by subhorizontal orientation with porous zones at the tops and bottoms of flows causing increased permeability and decreased resistivity in the horizontal direction. Current flow for the TEM soundings is completely horizontal, whereas for the SR soundings it is a combination of vertical and horizontal. Therefore the interpreted resistivity values would be expected to be less for the TEM results. Similar arguments can be made for the lower resistivity values for the induction log as compared to the short normal log (see Figure 16). The induction tool induces horizontally flowing currents, whereas the current flow for the short normal tool is primarily vertical. Resistivity anisotropy, therefore, accounts for the differences in the logs. The differences between the logs becomes less in very conductive zones which would tend to distort the current flow for the short normal tool into a more horizontal flow.

Discussion

Alteration minerals are commonly found in active and fossil hydrothermal systems [Steiner, 1968, Browne, 1970; Bailey et al., 1976; Keith and Muffler, 1978; Elders et al., 1979; Hulen and Nielson, 1986; Jakobsson and Moore, 1986]. While the minerals present are different for each system, commonly found minerals include smectite, illite, mixed layer illite-smectite, zeolite, calcite, chlorite, and epidote; there is usually a correlation between the minerals present and the temperature of the system [Krismannsdottir, 1976]. Smectite is found at temperatures as high as 200°C. Mixed layer illite-smectite and illite are found at higher temperatures. Zeolites are found at slightly lower temperatures with the maximum being around 150°C. Calcite is found over a very wide range of temperatures (50°C to 300°C). Epidote and chlorite are indicative of temperatures in excess of 200°C. The alteration minerals found in test holes Newberry 2 and GEO N-1 are among those commonly found in hydrothermal systems [Keith and Bargar, this issue].

Hydrothermal alteration has been known to produce conductivity anomalies in other geothermal systems. Zeolitic alteration on Réunion Island lowers the resistivity of basalts to as little as 1Ωm [Benderitter and Gérard, 1984]. In

Iceland, zeolites play a significant role where resistivities of less than 10□m have been observed in basalts [Flovenz et al., 1985]. Hydrothermally altered rhyolitic tuffs in Long Valley, California have resistivities in the range of 1Ωm to 10Ωm [Stanley et al., 1976].

Alteration minerals may be responsible for the conductivity anomalies at Newberry. Smectite occurs in Newberry 2 and GEO N-1 cores [Keith and Bargar, this issue]. Studies of the electrical properties of sedimentary rocks show that high cation exchange capacity materials such as clays dramatically reduce the bulk resistivity [Waxman and Smits, 1968]. Clays, such as smectite and illite, and zeolites are known to have high cation exchange capacities [Barrer, 1978; van Olphen and Fripat, 1979], and therefore provide a mechanism for producing the conductivity anomaly found at Newberry. The most direct evidence is given by Wright and Nielson [1986] who found that alteration zones in GEO N-1 core which were rich in smectite derived from ash flows had low resistivities (1.5-15Ωm) on the induction logs. Most of these conductive regions were at temperatures below 20°C demonstrating that altered rocks that are no longer at high temperatures can be very conductive.

Our interpretation of the data is that the conductive second layer mapped by the various electrical methods is largely the result of alteration. (High-temperature pore fluids may also contribute to the enhanced conductivity as seen in the caldera.) This, however, does not rule out or confirm that high-temperature pore fluids are present at greater depths outside the caldera. The caldera drilling results demonstrate that high-temperature fluids are present at depths greater than the smectite alteration, whereas on the flanks it is not clear that comparably high temperatures exist below the alteration.

The shallow conductivity anomaly on the west flank is underlain by a peak in the resistive third layer formed between the sharp rise in the electrical basement to the west and the drop in the basement under the western caldera rim to the east (see Figure 14). The drop under the caldera rim is based upon a single MT sounding and can not be considered conclusive. The structure shown, however, was derived using a resistivity for the second layer (8Ωm) which approximately results in the least drop. The suggestion of a peak in the resistive basement below the shallow, west-flank conductor may be geologically significant as it could indicate a region of intrusion that has caused enhanced hydrothermal alteration. Even though it is a one-point interpretation, if this hypothesis is correct, it supports the idea that the west-flank conductor is a geothermal target.

Our results point out a potential problem with the use of electrical techniques for geothermal exploration in the Cascades. Alteration of tuffs and ash deposits by hydrothermal fluids produces minerals that are very conductive even though they are presently not at high temperatures. Therefore, electrical methods can not be solely relied upon to give information about the presence of high-temperature pore fluids. Spectral induced polarization (SIP) or complex resistivity measurements provide a possible solution to this dilemma. SIP measures the electrical resistivity at several excitation frequencies. If the spectra of the altered and unaltered volcanic materials are different a discrimination can be made. There is some laboratory data indicating that the complex resistivity spectrum of clay minerals and barren rocks are significantly different to allow such a discrimination [Olhoeft, 1985]. In fact, hot volcanic rocks saturated with conductive pore fluids would be expected to have a small SIP response, whereas cold rocks with alteration minerals would have a large SIP response. Application of the SIP technique on a routine basis for geothermal exploration requires further laboratory and field studies.

From drilling we know that there are elevated temperatures below Newberry caldera, however, there is no direct evidence of magma. Because magma is conductive, it might be detectable using an electrical sounding method. Magma resistivities vary over a wide range depending upon dissolved water content. Burnham [1975] showed that the resistivity of siliceous melt varies between 1Ωm and 100Ωm at 1000°C for water contents of 1 to 4 percent; Wannamaker [1986] argued that a silicic melt in the mid-crust with 2.5 percent water would have a resistivity of about 4Ωm. Using resistivities in this range we have computed several simple models to illustrate possible detection of magma with MT soundings.

Figure 18 shows a generic four-layer model typical of those used to model the Newberry data set (dashed curve). We assume that magma exists in the resistive, electrical basement rocks (layer 3) and extends far enough laterally to permit the use of 1-D models. Three models with a magma layer having a conductance of 125S, 500S, and 1000S were calculated. When the magma layer has a conductance greater than 125S it would be distinguishable from the generic model. Thus for a resistivity of 4Ωm, a magma thickness of at least 500m is required. Decreasing the magma resistivity by a factor of two would reduce the layer thickness required for detection in the same proportion.

A more realistic view of the magma detection capability can be demonstrated with 3-D models. The most likely geologic situation would be a magma body of approximately 3-5km on a side at depths of 4-10km. Modelling of 3-D bodies by Newman et al. [1985] shows that magma detection by the MT method is very difficult in the presence of a lower-crustal conductor, such as that occurring at Newberry. The lower-crustal conductor appears to attenuate the response of a magma body. In addition, the models of Newman et al. did not have a conductive second layer as required by the Newberry data which would further mask the response of the magma body. In light of the numerous distorting factors, we believe that it will be very difficult to detect a discrete 3-D magma body using MT measurements. An extensive survey with very high-power TEM equipment capable of penetrating to over 5km depth is probably the optimal way of electrically detecting any magma bodies beneath Newberry.

Newberry Volcano sits atop a significant rise in the resistive electrical basement which we interpret to be intrusive material. This hypothesis is supported by the gravity data (see Figure 14), which mimics the shape of the electrical basement. Williams and Finn [1985] model the residual Bouguer gravity anomaly as a high-density intrusive body. The gravity minimum inside the caldera is due to low-density caldera fill. Gettings and Griscom [this volume] have obtained similar results.

Part of the resistive structure below the volcano may be due to a sealed, vapor-dominated geothermal system. High-temperature alteration minerals such as chlorite and epidote as well as silica seen in the bottom of Newberry 2 tend to clog pore spaces and seal permeability. The presence of steam and high-density, low-porosity intrusive rocks would overlap the high basement resistivity values [Zohdy et al., 1973]. Pods of magma, too small to be detectable by surface geophysical techniques, could exist within the high-resistivity intrusive complex. Only drilling can confirm this hypothesis.

Conclusions

Newberry Volcano is underlain at depths of about 2km by a resistive basement. The resistive basement may be intrusive rocks [Williams and Finn, 1985; Gettings and Griscom, this volume]. Our geoelectrical data do not provide any evidence suggesting the presence of magma. The data would allow for, but is not diagnostic of, magma in small discontinuous pods or for a layer whose conductance is less than 125S. Overlying the resistive basement is an extensive

conductor that we interpret to be the result of regional hydrothermal alteration of volcanic ash. While elevated temperatures inside the caldera contribute to the conductivity anomaly, on the flanks of the volcano temperatures are significantly lower and do not influence the conductivity. The areal extent of the conductor indicates that alteration is widespread. The conductive zone is shallowest inside the caldera and on the west flank suggesting that these are regions where hydrothermal activity has been the most intense. Drilling has confirmed the existence of a hydrothermal system in the caldera while test holes outside the caldera have found low temperatures. Alteration minerals such as smectite, which has been found in all drill holes, are the probable cause of the conductivity anomaly.

As conductivity anomalies can be caused by alteration minerals that form at low temperatures, this poses an exploration problem when using electrical geophysical methods. The problem of low-temperature conductors is probably ubiquitous to the Cascades as much of the area is underlain by sediments and ash-rich volcanics that can alter to smectite at low temperatures. Spectral induced polarization measurements may provide a means of determining the presence and type of alteration, and thereby characterize exploration targets. Further work on this hypothesis is needed.

Acknowledgement

This work was funded in part by the Department of Energy under Interagency Agreement DE-A101-70RA50294. Permission to conduct the field work was granted by the Deschutes National Forest, Bend, Oregon.

References

Anderson, W. L., Nonlinear least-squares inversion of transient soundings for a central induction loop system (program NLSTCI), Open-File Report 82-1129, 85 pp., U.S. Geol. Surv., Denver, CO, 1982.

Bailey, R., A., G. B. Dalrymple, and M. A. Lanphere, Volcanism, structure, and geochronology of Long Valley Caldera, Mono County, California, J. Geophys. Res., 81, 725-744, 1976.

Bargar, K. E., and T. E. C. Keith, Hydrothermal alteration mineralogy in Newberry 2 drill core, Newberry Volcano, Oregon, Open-File Report 84-92, 62 pp., U.S. Geol. Surv., Menlo Park, CA, 1984.

Bargar, K. E., and T. E. C. Keith, Hydrothermal mineralization in GEO N-1 drill hole, Newberry Volcano, Oregon, Open-File Report 86-440, 18 pp., U.S. Geol. Surv., Menlo Park, CA, 1986.

Barrer, R. M., Cation-exchange equilibria in zeolites and feldspathoids, in Natural Zeolites--Occurrence, Properties, Use, edited by L. B. Sand and F. A. Mumpton, pp. 385-395, Pergamon Press, Oxford, 1978.

Benderitter, Y., and A. Gérard, Geothermal study of Réunion Island: audiomagnetotelluric survey, J. Vol. Geotherm. Res., 20, 311-332, 1984.

Berdichevsky, M. N., and V. I. Dimetriev, Basic principles of interpretation of magnetotelluric sounding curves, in Geoelectric and Geothermal Studies, edited by A. Adam, pp. 165-221, Academai Kiado, Budapest, 1976.

Bisdorf, R. J., Schlumberger soundings near Newberry Caldera, Oregon, Open-File Report 83-825, 51 pp., U.S. Geol. Surv., Denver, CO, 1983.

Bisdorf, R. J., Schlumberger sounding results over the Newberry Volcano area, Oregon, Trans. Geothermal Resources Counc., 9, Part II, pp. 389-394, Geothermal Resources Counc., Davis, CA, 1985.

Black, G. L., G. R. Priest, and N. M. Woller, Temperature data and drilling history of the Sandia National Laboratories well at Newberry caldera, Oregon Geology, 46, 7-9, 1984.

Browne, P. R. L., Hydrothermal alteration as an aid in investigating geothermal fields, Geotherm. Spec. Issue 2, 564-570, 1970.

Burnham, C. W., Water and magmas; a mixing model, Geochemica et Cosmochemica Acta, 39, 1077-1084, 1975.

Elders, W. A., J. R. Hoagland, S. D. McDowell, and J. M. Cobo, Hydrothermal mineral zones in the geothermal reservoir of Cerro Prieto, Geothermics, 8, 201-209, 1979.

Fitterman, D. V., Time-domain electromagnetic soundings of Newberry Volcano, Deschutes County, Oregon, Open-File Report 83-832, 57 pp., U.S. Geol. Surv., Denver,CO, 1983.

Fitterman, D. V., and D. K. Neev, Transient sounding investigation of Newberry Volcano, Oregon, Trans. Geothermal Resources Counc., 9, Part II, pp. 407-410, Geothermal Resources Counc., Davis, CA, 1985.

Fitterman, D. V., D. K. Neev, J. A. Bradley, and C. T. Grose, More time-domain electromagnetic soundings of Newberry Volcano, Deschutes County, Oregon, Open-File Report 85-451, 76 pp., U.S. Geol. Surv., Denver, CO, 1985.

Fitterman, D. V., and M. T. Stewart, Transient electromagnetic sounding for groundwater, Geophysics, 51, 995-1005, 1986.

Flóvenz, O., G., L. S. Georgsson, and K. Arnason, Resistivity structure of the upper crust in Iceland, J. Geophys. Res., 90, 10,136-10,150, 1985.

Gettings, M. E., and Andrew Griscom, Gravity model studies of Newberry Volcano, Oregon, J. Geophys. Res., this issue.

Hulen, J. B., and D. L. Nielson, Hydrothermal alteration in the Baca geothermal system, Redondo Dome, Valles Caldera, New Mexico, J. Geophys. Res, 91, 1867-1886, 1986.

Jakobsson, S. P., and J. G. Moore, Hydrothermal minerals and alteration rates at Surtsey volcano, Iceland, Bull. Geol. Soc. Am., 97, 648-659, 1986.

Jones, A. G., Static-shift of magnetotelluric data and its removal in a sedimentary basin environment, Geophysics, submitted 1987.

Kaufman, A. A., and G. R. Keller, Frequency and Transient Sounding, 685 pp., Elsevier, Amsterdam, 1983.

Keith, T. E. C., and K. E. Bargar, Petrology and hydrothermal convection of Newberry 2 drill core, Oregon, J. Geophys. Res., this issue.

Keith, T. E. C., and L. J. P. Muffler, Minerals produced during cooling and hydrothermal alteration of ash flow tuff from Yellowstone drill hole Y-5, J. Volcanol. Geotherm. Res., 3, 373-402, 1978.

Keith, T. E. C., and L. J. P. Muffler, Minerals produced during cooling and hydrothermal alteration of ash flow tuff from Yellowstone drill hole Y-5, J. Volcanol. Geotherm. Res., 3, 373-402, 1978.

Keith, T. E. C., R. H. Mariner, K. E. Bargar, W. C. Evans, and T. S. Presser, Hydrothermal alteration in Oregon's Newberry Volcano No. 2--fluid chemistry and secondary-mineral distribution, Geothermal Resources Council Bulletin, 13, 9-17, 1984.

Kristmannsdottir, H., Hydrothermal alteration of basaltic rocks in Icelandic geothermal areas, Proc. 2nd U.N. Symp. Dev. Use Geotherm. Resour., 441-445, 1976.

Larsen, J. C., Low-frequency (0.1-6 cpd) electromagnetic study of the deep mantle electric conductivity beneath the Hawaiian Islands, Geophys. J. Royal Astronom. Soc., 43, 17-46, 1975.

MacLeod, N. S., and E. A. Sammel, Newberry volcano, Oregon--a Cascade Range geothermal prospect, California Geology, 35, 235-244, 1982.

MacLeod, N. S., and D. R. Sherrod, Geologic evidence for a magma chamber beneath Newberry Volcano, Oregon, J. Geophys. Res., this issue.

MacLeod, N. S., D. R. Sherrod, and L. A. Chitwood, Geologic map of Newberry volcano, Deschutes, Klamath, and Lake Counties, Oregon, Open-File Report 82-847, 27 pp., U.S. Geol. Surv., Vancouver, WA, 1982.

MacLeod, N. S., G. W. Walker, and McKee, E. H., Geothermal significance of eastward increase in age of upper Cenozoic rhyolitic domes in southeast Oregon, Proc. Second United Nations Symposium on the development and use of geothermal resources, 1, 465-474, 1975.

MacLeod, N. S., D. R. Sherrod, L. A. Chitwood, and E. H. McKee, Newberry volcano, Oregon, in Guides to some volcanic terranes in Washington, Idaho, Oregon, and Northern California, edited by D. A. Johnston and J. Donnelly-Nolan, pp. 85-91, Circular 838, U.S. Geol. Surv., Reston, VA, 1981.

Nabighian, M. N., Quasi-static transient response of a conducting half-space--an approximate representation, Geophysics, 44, 1700-1705, 1979.

Newman, G. A., P. W. Wannamaker, and G. W. Hohmann, On the detectability of crustal magma chambers using the magnetotelluric method, Geophysics, 50, 1135-1143, 1985.

Olhoeft, G. R., Electrical properties of granite with implications for the lower crust, J. Geophys. Res., 86, 931-936, 1981.

Olhoeft, G. R., Low-frequency electrical properties, Geophysics, 50, 2492-2503, 1985.

Park, S. K., Distortion of magnetotelluric sounding curves by three-dimensional structures, Geophysics, 50, 785-797, 1985.

Parkhomenko, E. I., Electrical Properties of Rocks, 314 pp., Plenum, New York, 1967.

Sammel, E. A., Results of test drilling at Newberry Volcano, Oregon, Geothermal Resources Council Bull., 10, 3-8., 1981.

Sammel, E. A., and R. W. Craig, Hydrology of Newberry Volcano caldera, Oregon, Water Resources Investigation Report 83-4091, 52 pp., U.S. Geol. Surv., Menlo Park, CA, 1983.

Spies, B. R., and D. E. Eggers, The use and misuse of apparent resistivity in electromagnetic methods, Geophysics, 51, 1462-1479, 1986.

Stanley W. D., Field procedures to resolve 3-D effects in magnetotellurics, (abstract), presented at Workshop in Magnetotellurics sponsored by U. S. Geological Survey, St. Helena, California, 1980.

Stanley, W. D., A regional magnetotelluric survey of the Cascades Mountains region, Open-File Report 82-126, 20 pp., U.S. Geol. Surv., Denver, CO, 1982.

Stanley, W. D., Regional and local geoelectrical structures in the Cascades and their role in geothermal and volcanic hazard assessment, Eos, 64, 887, 1983.

Stanley,W. D., D. B. Jackson, and Adel A. R. Zohdy, Deep electrical investigations in the Long Valley geothermal area, California, J. Geophys. Res., 81, 810-820, 1976.

Stanley,W. D., J. E. Boehl, F. X. Bostick, Jr., and H. W. Smith, Geothermal significance of MT sounding in the eastern Snake River-Yellowstone region, J. Geophys. Res., 82, 2501-2514, 1977.

Steiner, A., Clay minerals in hydrothermally altered rocks at Wairakei, New Zealand, Clays Clay Miner., 16, 193-213, 1968.

Swanberg, C. A., and J. Combs, Geothermal drilling in the Cascade Range: preliminary results from a 1387m core hole, Newberry Volcano, Oregon, Eos, 67, 578-579, 1986.

Swanberg, C. A., W. C. Walkey, and Jim Combs, Core hole Drilling and the "rain curtain" phenomenon at Newberry Volcano Oregon, J. Geophys. Res., this issue.

van Olpehn, H., and J. J. Fripat, Data Handbook for Clay Materials and Other Non-Metallic Minerals, 346 pp., Pergamon Press, Oxford, 1979.

Vozoff, K., The magnetotelluric method in the exploration of sedimentary basins, Geophysics, 37, 98-141, 1972.

Wannamaker, P. E., Electrical conductivity of water-undersaturated crustal melting, J. Geophys. Res., 91, 6321-6328, 1986.

Waxman, M. H., and L. J. M. Smits, Electrical conductivities in oil-bearing shaly sands, Soc. Petr. Eng. J., Trans. AIME, 243, 107-122, 1968.

Williams, D. L., and C. Finn, Analysis of gravity data in volcanic terrain and gravity anomalies and subvolcanic intrusions in the Cascade Range, U.S.A., and at other selected volcanoes, in The Utility of Regional Gravity and Magnetic Anomaly Maps, edited by W. J. Hinze, pp. 361-374, Society of Exploration Geophysicists, Tulsa, Okla., 1985.

Wright, P. M., and D. L. Nielson, Electrical resistivity anomalies at Newberry Volcano, Oregon; comparison with alteration mineralogy in GEO corehole N-1, Trans. Geotherm. Res. Coun., 10, pp. 247-252, 1986.

Zhang, P., R. G. Roberts, L. B. Pedersen, Magnetotelluric strike rules, Geophysics, 52, 267-278, 1987.

Zohdy, A. A. R., A computer program for the automatic interpretation of Schlumberger sounding curves over horizontally layered media, NTIS Report PB-232 703/AS, 25 pp., National Technical Information Service, Springfield, VA, 1973.

Zohdy, A. A. R., Automatic interpretation of Schlumberger sounding curves using modified Dar Zarrouk functions, Bulletin 1313-E, 39 pp., U.S. Geol. Surv., Denver, CO, 1975.

Zohdy, A. A. R., L. A. Anderson, and L. J. P. Muffler, Resistivity, self-potential, and induced-polarization surveys of a vapor-dominated geothermal system, Geophysics, 38, 1130-1144, 1973.

Zohdy, A. A. R., and R. J. Bisdorf, Schlumberger soundings in the Medicine Lake are, California, Open-File Report 82-887, 162 pp., U.S. Geol. Surv., Denver, CO, 1982.

R. J. Bisdorf, D. V. Fitterman, and W. D. Stanley, U.S. Geological Survey, Box 25046, MS 964, Denver Federal Center, Denver, CO 80225.

Figure Captions

Figure 1 Regional geologic map showing location of Newberry volcano. Line A-A' is the location of the MT transect shown in Figure 8.

Figure 2 Map showing the location of the magnetotelluric (circles), transient electromagnetic (squares), and Schlumberger resistivity (triangles) soundings. Line B-B' is the location of the cross section shown in Figure 14. The filled in station location symbols correspond to stations used to make the cross section. The inferred caldera ring faults of MacLeod et al. [1982] is shown as a heavy dashed line. The locations of the USGS and GEO-Operator test wells are shown (ticked circles). The elevation contours are in meters. The shaded areas are Paulina Lake and East Lake.

Figure 3 Example MT sounding curves from the western part of the study area. Triangles are ρ_{xy} and squares ρ_{yx} resistivities and phases respectively. The 1-D model curves for these soundings are shown by the solid lines. The inset map shows the sounding locations (circles) and wells (ticked circles) relative to the caldera ring fracture (heavy dashed lines) and lakes (shaded area).

Figure 4 Examples of MT sounding curves from the area close to the caldera that show the effect of near surface inhomogeneities as evidenced by the parallel separation of the curves for the x-direction (triangles) and the y-direction (squares). The inset map is similar to the one in Figure 3.

Figure 5 Transient electromagnetic sounding late-stage apparent resistivity curves from three different locations. The circles are the observed values, and the solid line is the computed model. The inset map is similar to the one in Figure 3. Station symbols are squares.

Figure 6 Interpreted layer resistivities for the three soundings shown in Figure 5.

Figure 7 Schlumberger apparent resistivity sounding curves (symbols are observations and the smooth curves are the computed model) and interpretations (stair-step curves) for three locations. The inset map in similar to the one in Figure 3. Station symbols are triangles.

Figure 8 MT transect based on 1-D interpretations across the Cascades Range going through Newberry Volcano. The transect location is shown in Figure 1.

Figure 9 Map of interpreted Schlumberger resistivity in ohm-meters at a depth of 250m. Triangles are station locations. The caldera ring fracture (heavy dashed line), wells (ticked circles), and the lakes (shaded area) are shown.

Figure 10 Interpreted depth in meters to the conductive second layer from TEM data. Squares are station locations. The caldera ring fracture (heavy dashed line), wells (ticked circles), and the lakes (shaded area) are shown.

Figure 11 Interpreted resistivity in ohm-meters of the conductive second layer from TEM data. Squares are stations locations. The caldera ring fracture (heavy dashed line), wells (ticked circles), and the lakes (shaded area) are shown.

Figure 12 Interpreted resistivity in ohm-meters of the conductive second layer from MT data. Circles are station locations. The caldera ring fracture (heavy dashed line), wells (ticked circles), and the lakes (shaded area) are shown.

Figure 13 Interpreted depth in kilometers to the electrical basement (resistive layer 3) from MT data. Circles are station locations. The caldera ring fracture (heavy dashed line), wells (ticked circles), and the lakes (shaded area) are shown.

Figure 14 Composite geoelectrical cross-section made using Schlumberger, transient EM, and MT data. The data set used to determine the layer depths is marked. The numbers are interpreted resistivities in ohm-m. The first-layer resistivities were determined from SR data. The conductive second-layer resistivities were determined from the TEM data (numbers just below TEM conductor) and MT data (numbers just above MT electrical basement). The residual Bouguer gravity profile of Williams and Finn [1985] is shown below.

Figure 15 Interpreted layer resistivity-depth functions for surface electrical soundings (MT-56, TEM-3, and SR-1) and measured temperature for U.S.G.S. test hole Newberry 2. Zones of smectite alteration are shown by the bar on the temperature plot [Keith and Bargar, this volume].

Figure 16 Interpreted layer resistivity-depth functions for soundings (TEM-37, MT-N30, and SR-204) and measured temperature for GEO Operator N-1 test hole. The deep induction (IDL) and short normal (SN) well logs are shown for comparison. Zones of smectite alteration are shown by the bar on the temperature plot [Keith and Bargar, 1986].

Figure 17 Interpreted layer resistivity-depth functions for soundings (TEM-53, MT-N22, and SR-214) and measured temperature for GEO Operator N-3 test hole.

Figure 18 Layered-earth MT models showing the effect of a magma layer of different thickness and resistivity (curves A, B, and C). The dashed curve is for a typical four-layer model used to fit the Newberry data.

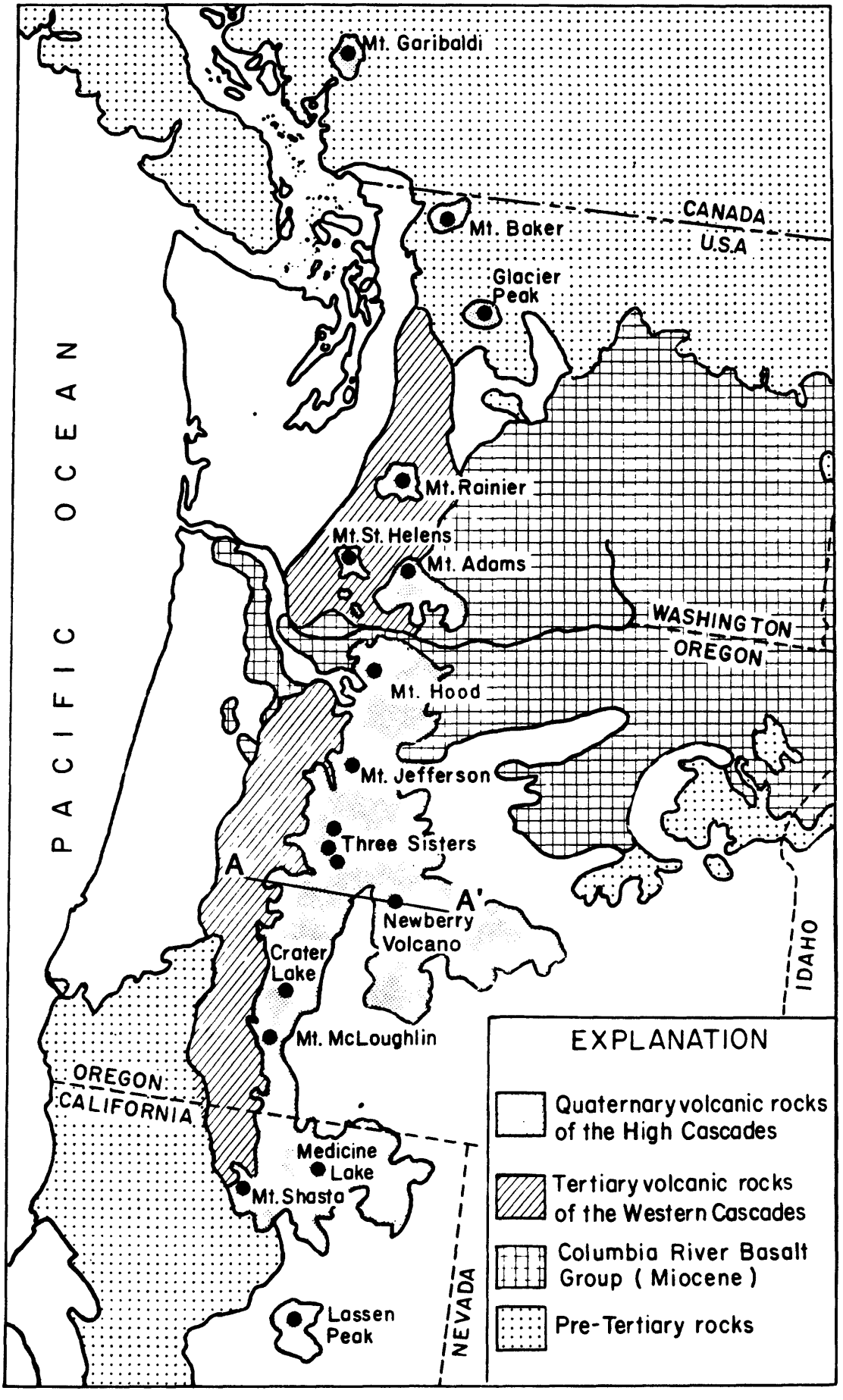
Mt. Garibaldi
CANADA
U.S.A
Mt. Baker
Glacier Peak
PACIFIC OCEAN
Mt. Rainier
Mt. St. Helens
Mt. Adams
WASHINGTON
OREGON
Mt. Hood
Mt. Jefferson
Three Sisters
A
A'
Newberry Volcano
Crater Lake
IDAHO
Mt. McLoughlin
OREGON
CALIFORNIA
Medicine Lake
Mt. Shasta
Lassen Peak
NEVADA
EXPLANATION
Quaternary volcanic rocks of the High Cascades
Tertiary volcanic rocks of the Western Cascades
Columbia River Basalt Group (Miocene)
Pre-Tertiary rocks

Figure 1

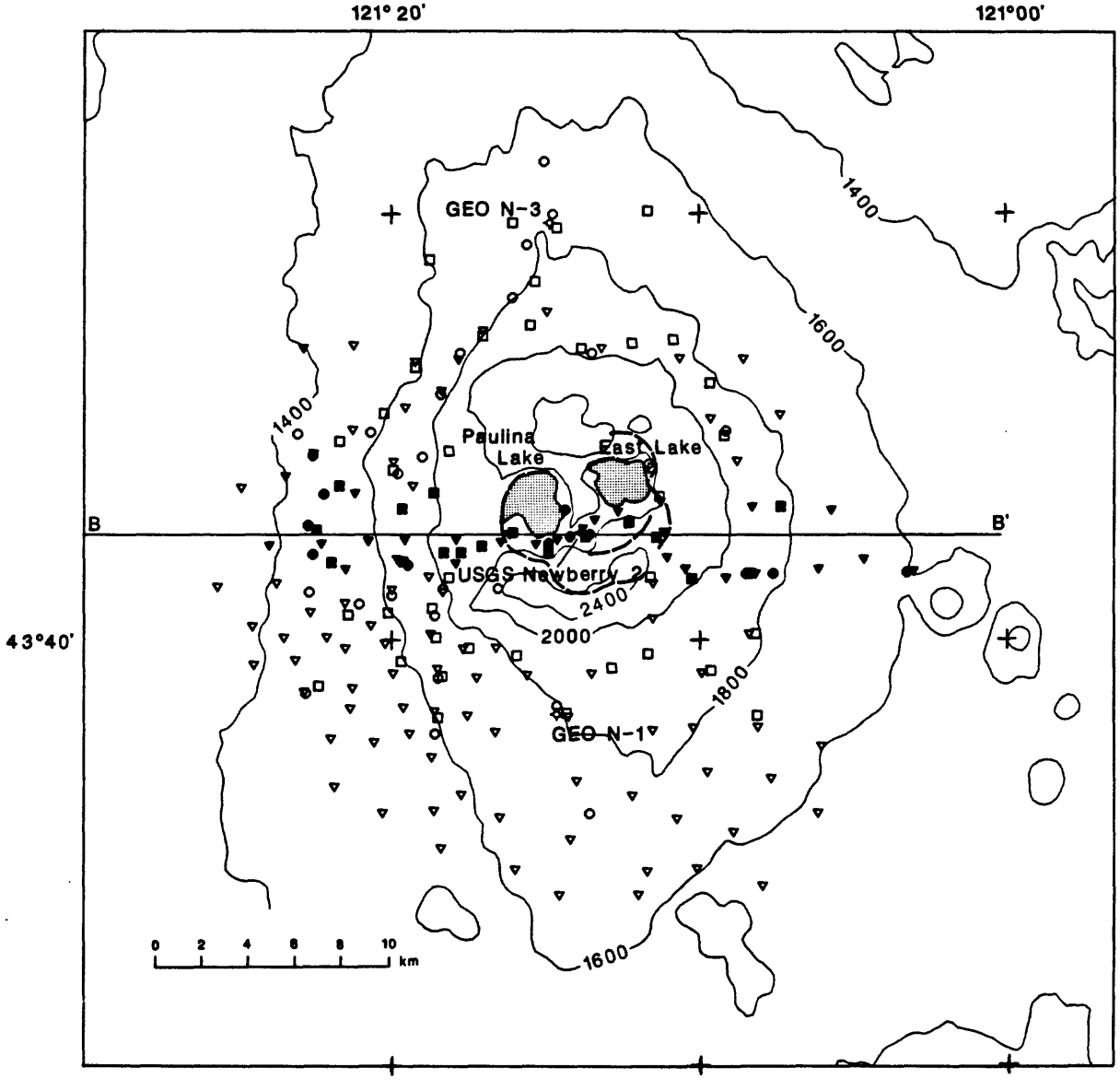
121° 20'
121°00'
43°40'
GEO N-3
Paulina Lake
East Lake
USGS Newberry 2
GEO N-1
B
B'
1400
1600
1800
2000
2400
0 2 4 6 8 10
km

2

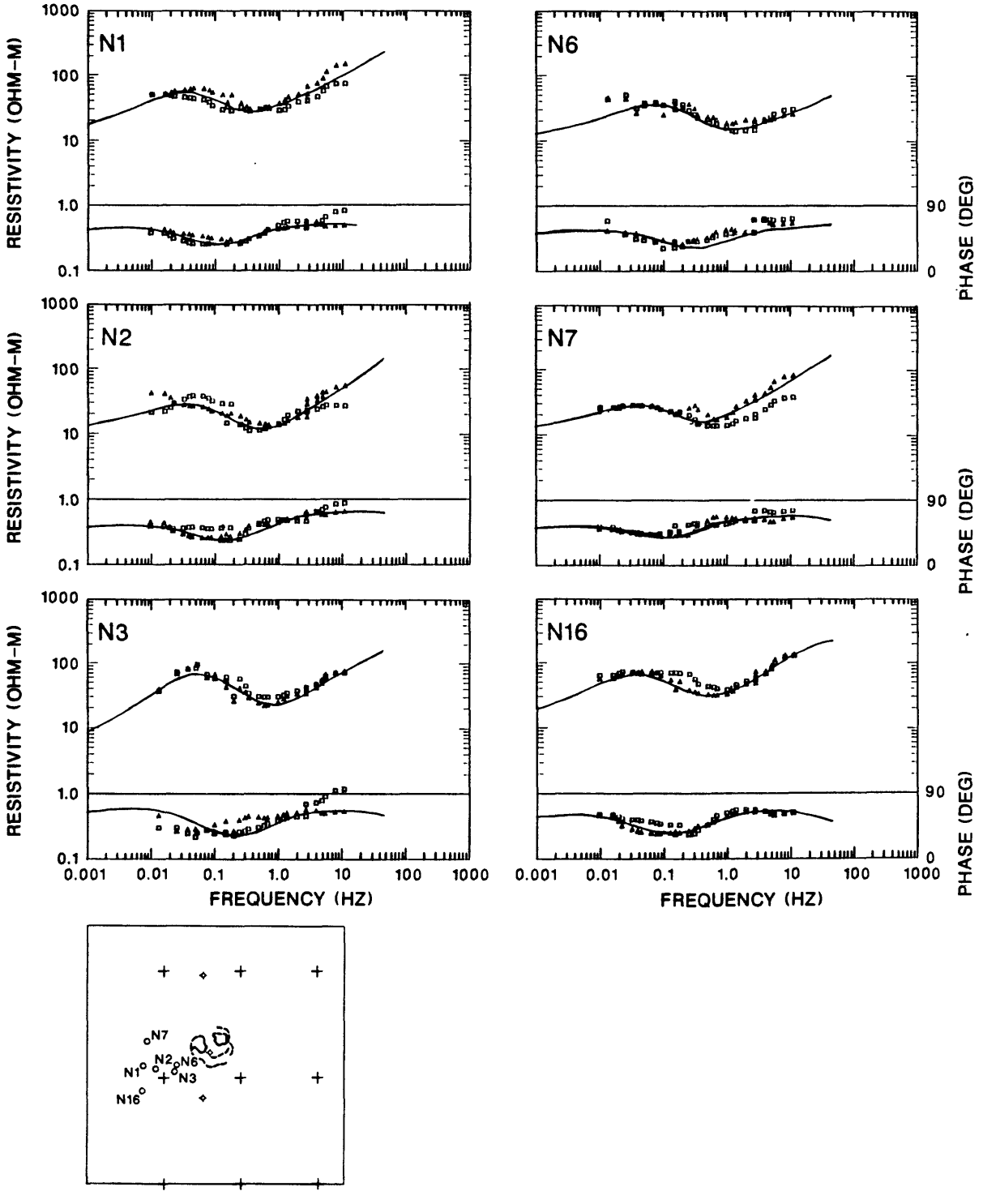
N1
N6
N2
N7
N3
N16
RESISTIVITY (OHM-M)
PHASE (DEG)
1000
100
10
1.0
0.1
90
0
0.001
0.01
0.1
1.0
10
100
1000
FREQUENCY (HZ)
N7
N2
N6
N1
N3
N16

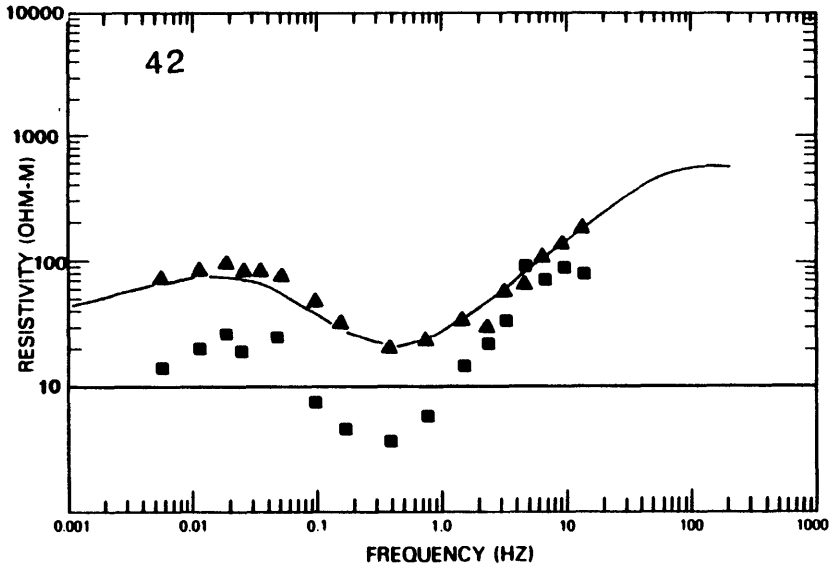
42
RESISTIVITY (OHM-M)
10000
1000
100
10
0.001
0.01
0.1
1.0
10
100
1000
FREQUENCY (HZ)

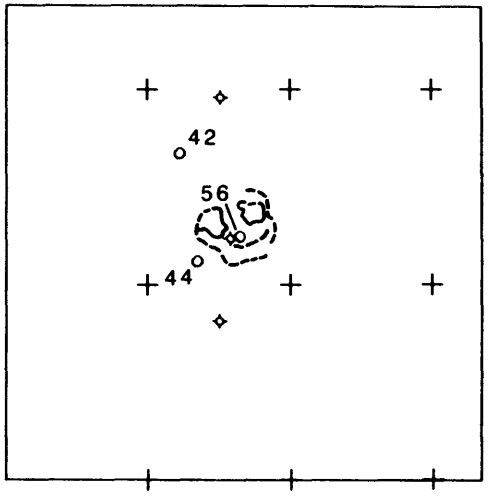
42
56
44

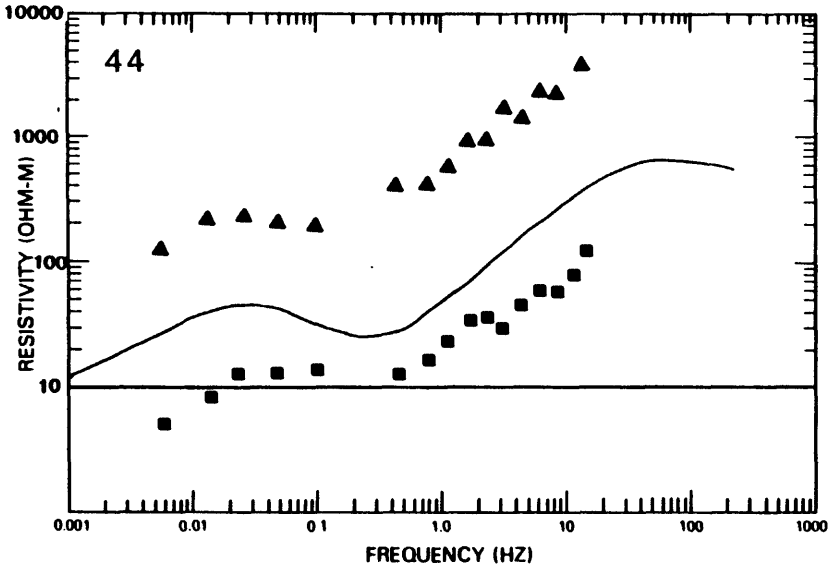
44
RESISTIVITY (OHM-M)
10000
1000
100
10
0.001
0.01
0.1
1.0
10
100
1000
FREQUENCY (HZ)

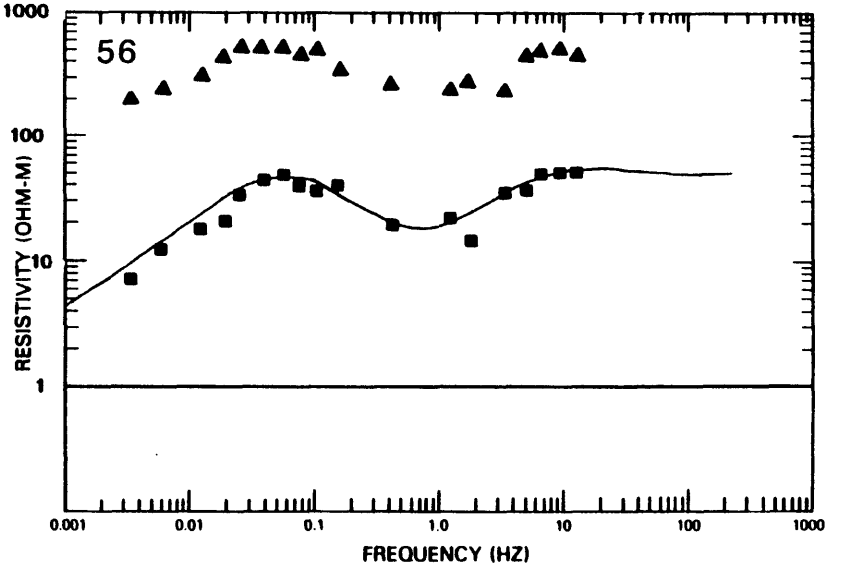
56
RESISTIVITY (OHM-M)
1000
100
10
1
0.001
0.01
0.1
1.0
10
100
1000
FREQUENCY (HZ)

3/

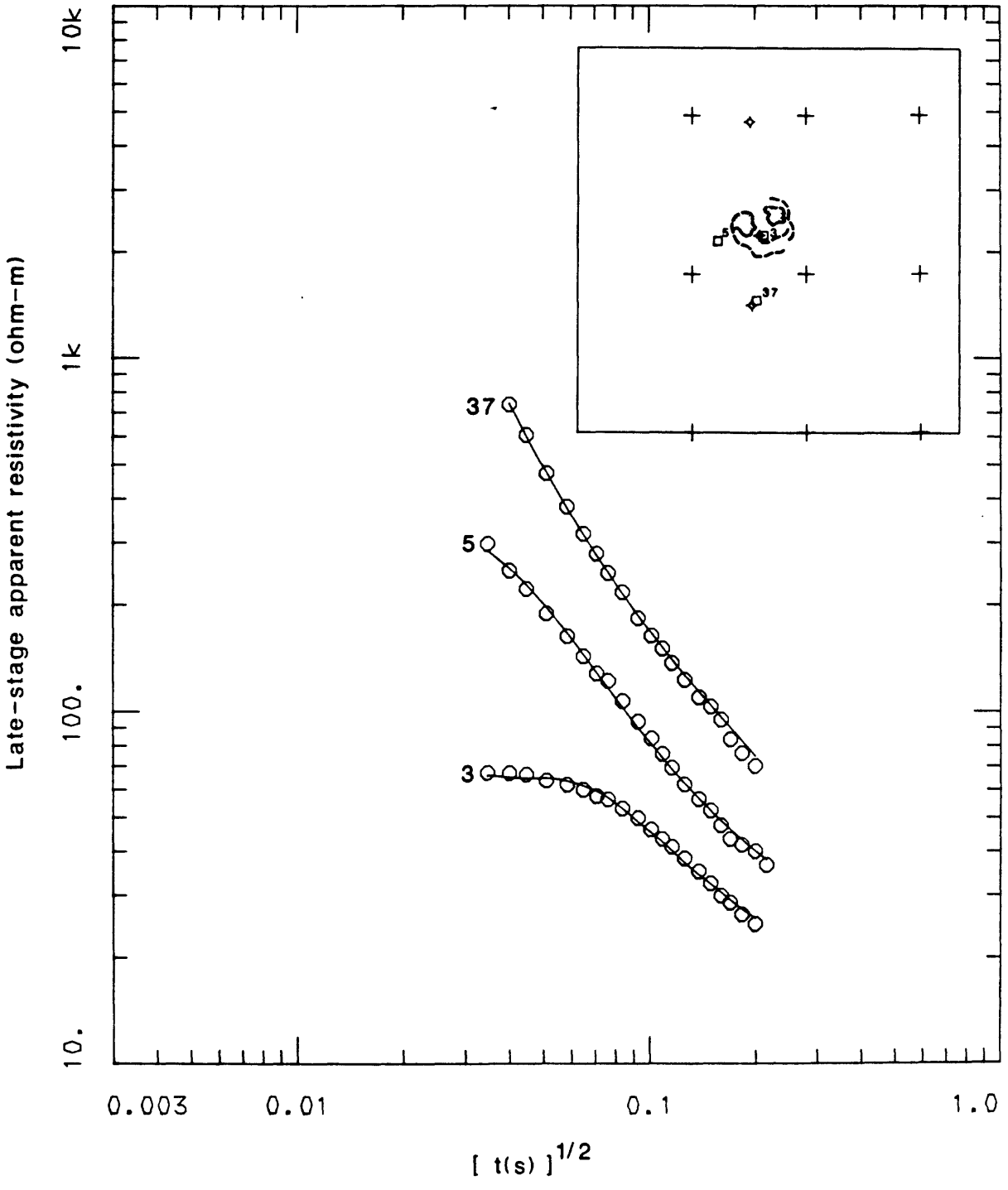
Late-stage apparent resistivity (ohm-m)
10k
1k
100.
10.
0.003
0.01
0.1
1.0
[t(s)]1/2
37
5
3

5

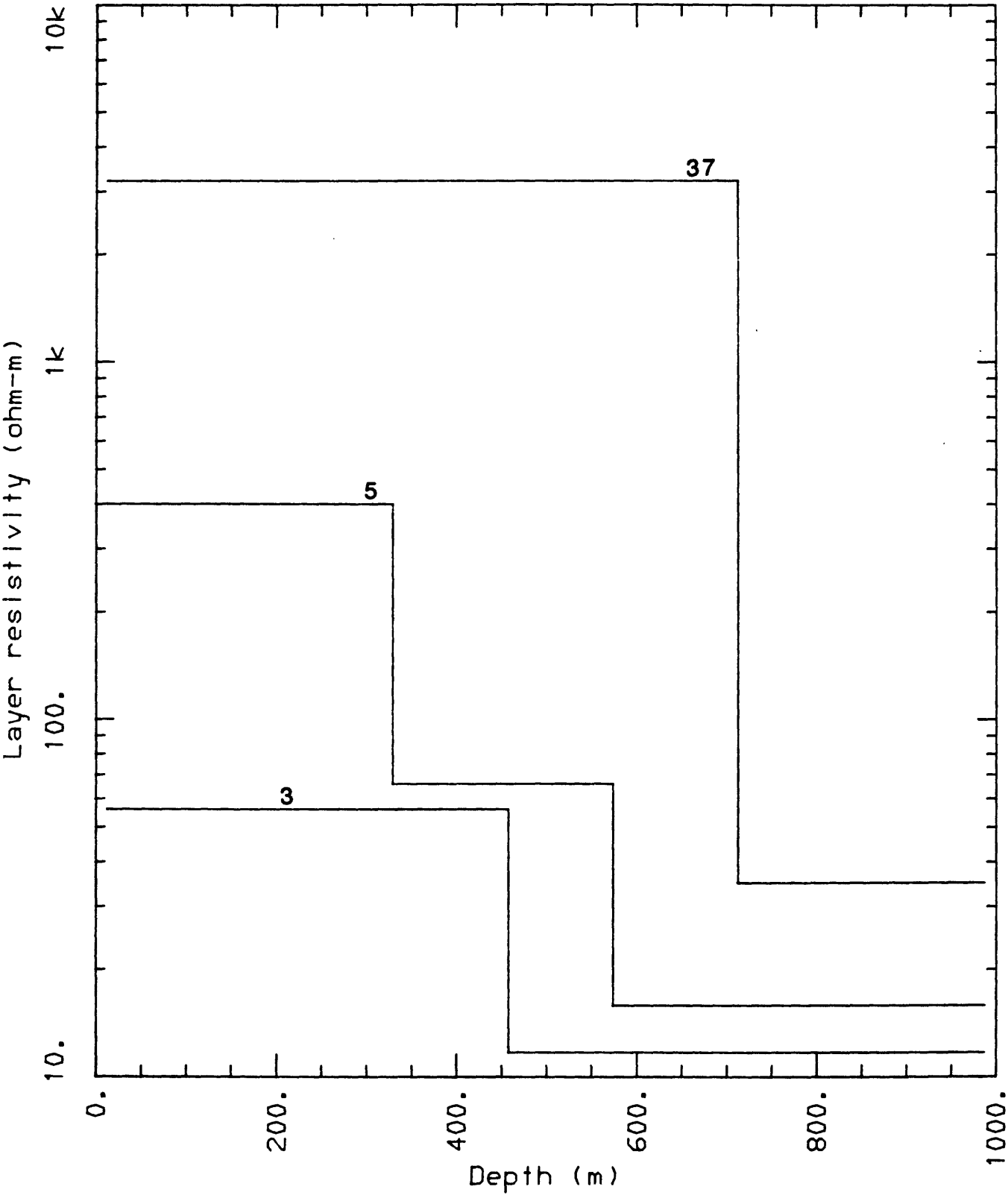
Layer resistivity (ohm-m)
10k
1k
100.
10.
37
5
3
0.
200.
400.
600.
800.
1000.
Depth (m)

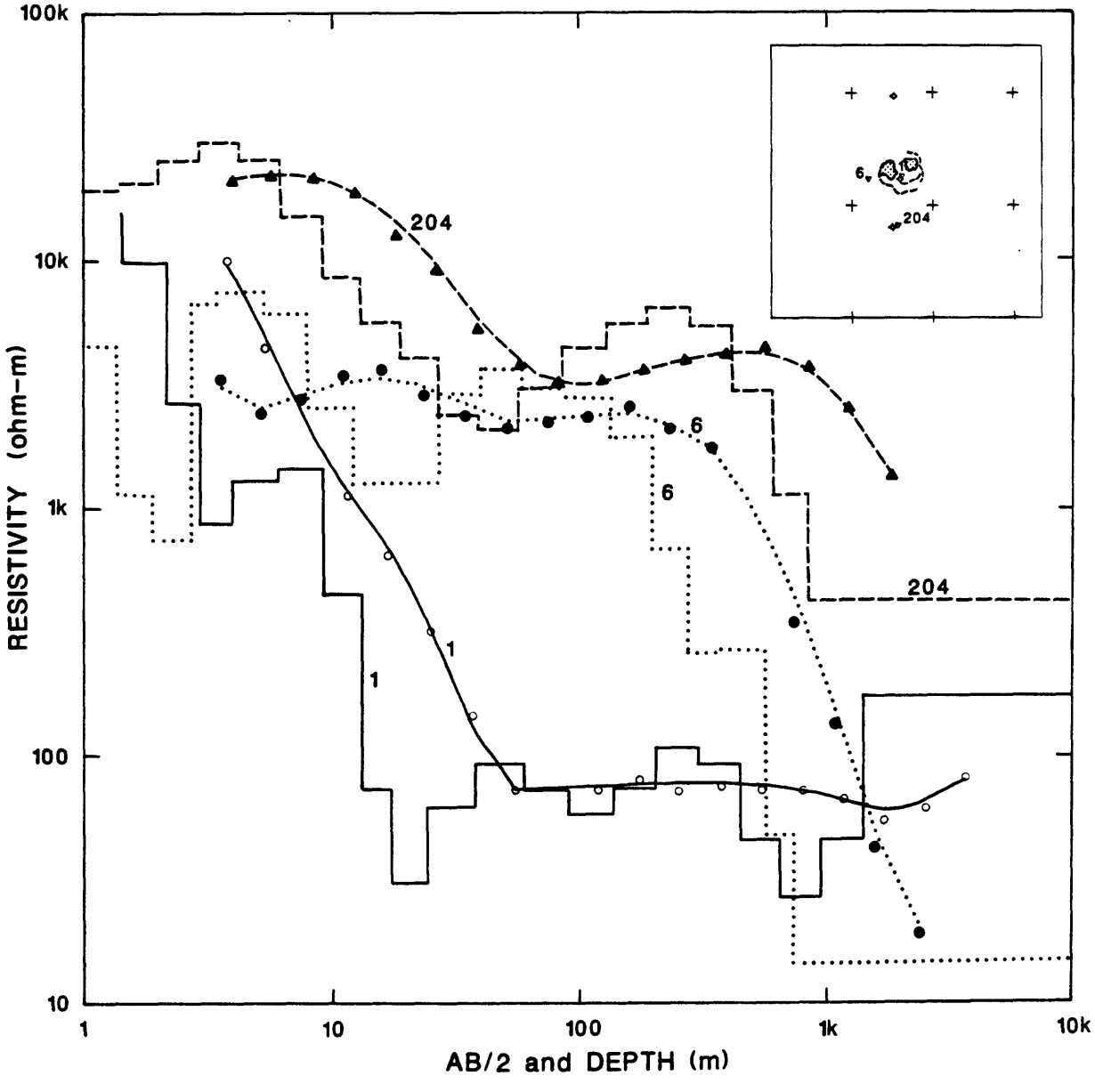
100k
10k
1k
100
10
RESISTIVITY (ohm-m)
1
10
100
1k
10k
AB/2 and DEPTH (m)
204
6
1
204
6
1
6
204

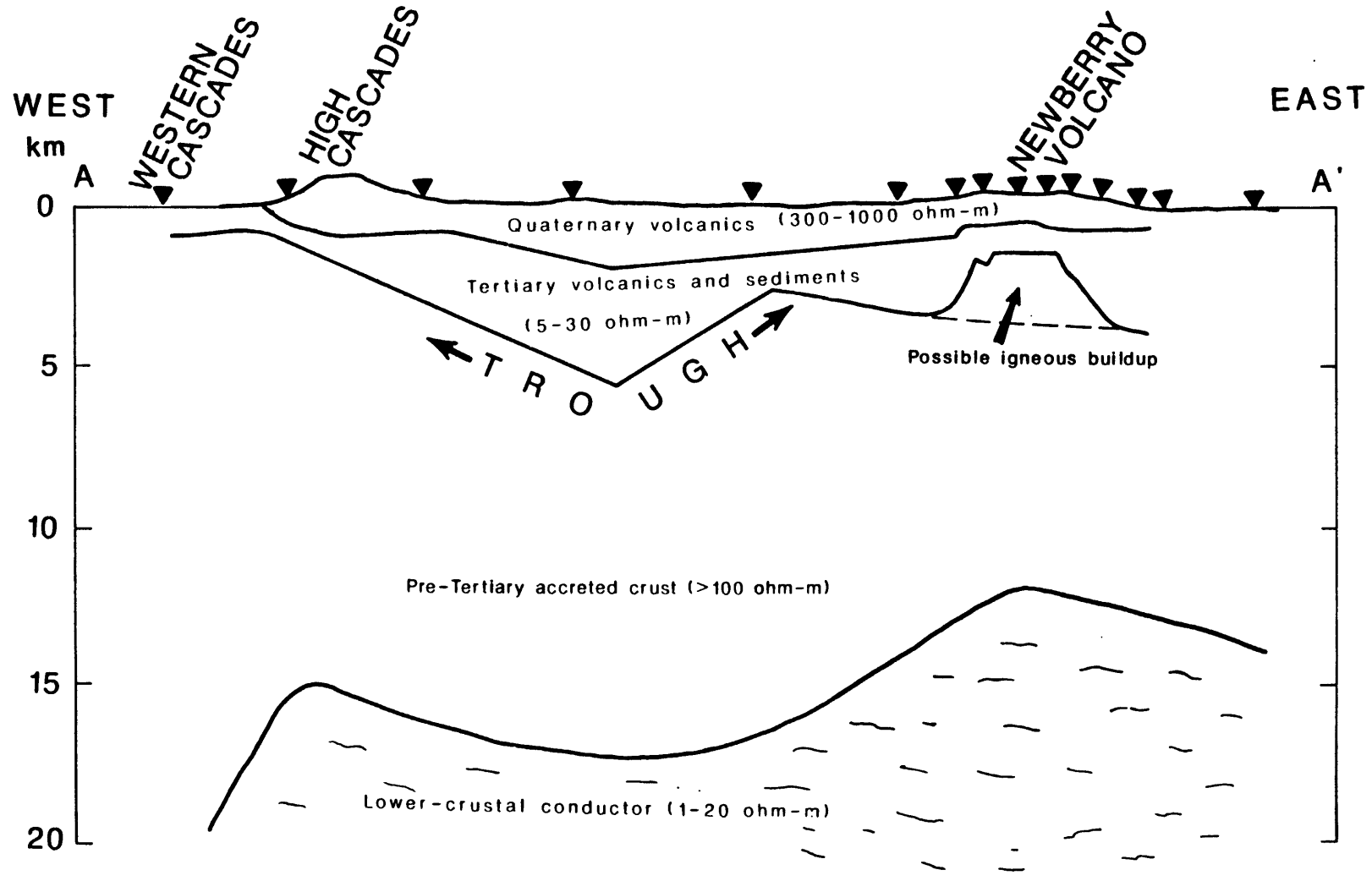
WEST
km
A
WESTERN CASCADES
HIGH CASCADES
NEWBERRY VOLCANO
EAST
A'
0
5
10
15
20
Quaternary volcanics (300-1000 ohm-m)
Tertiary volcanics and sediments
(5-30 ohm-m)
TROUGH
Possible igneous buildup
Pre-Tertiary accreted crust (>100 ohm-m)
Lower-crustal conductor (1-20 ohm-m)

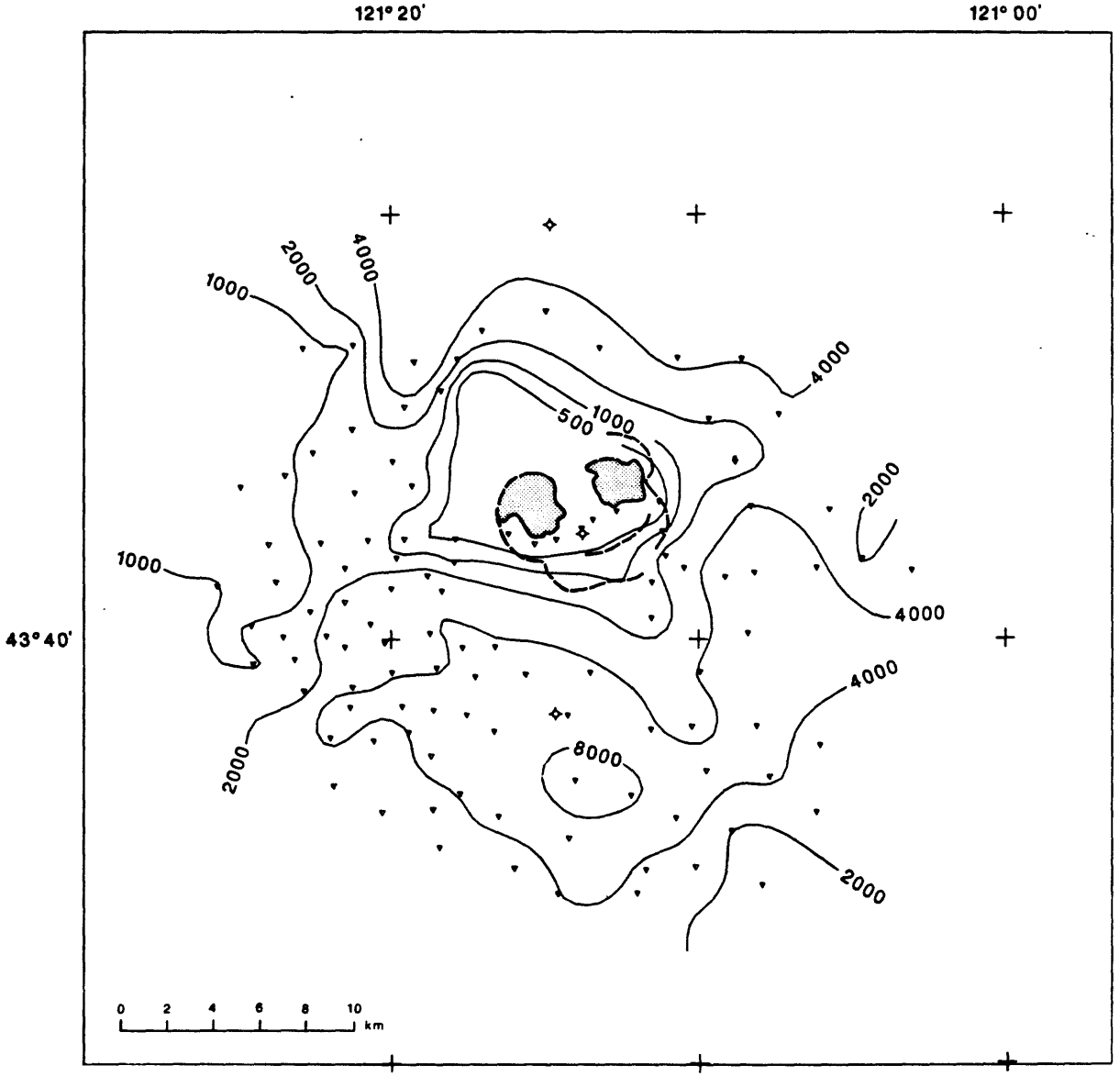
121° 20'
121° 00'
43° 40'
1000
2000
4000
500
1000
4000
2000
1000
4000
2000
4000
8000
2000
0 2 4 6 8 10
km

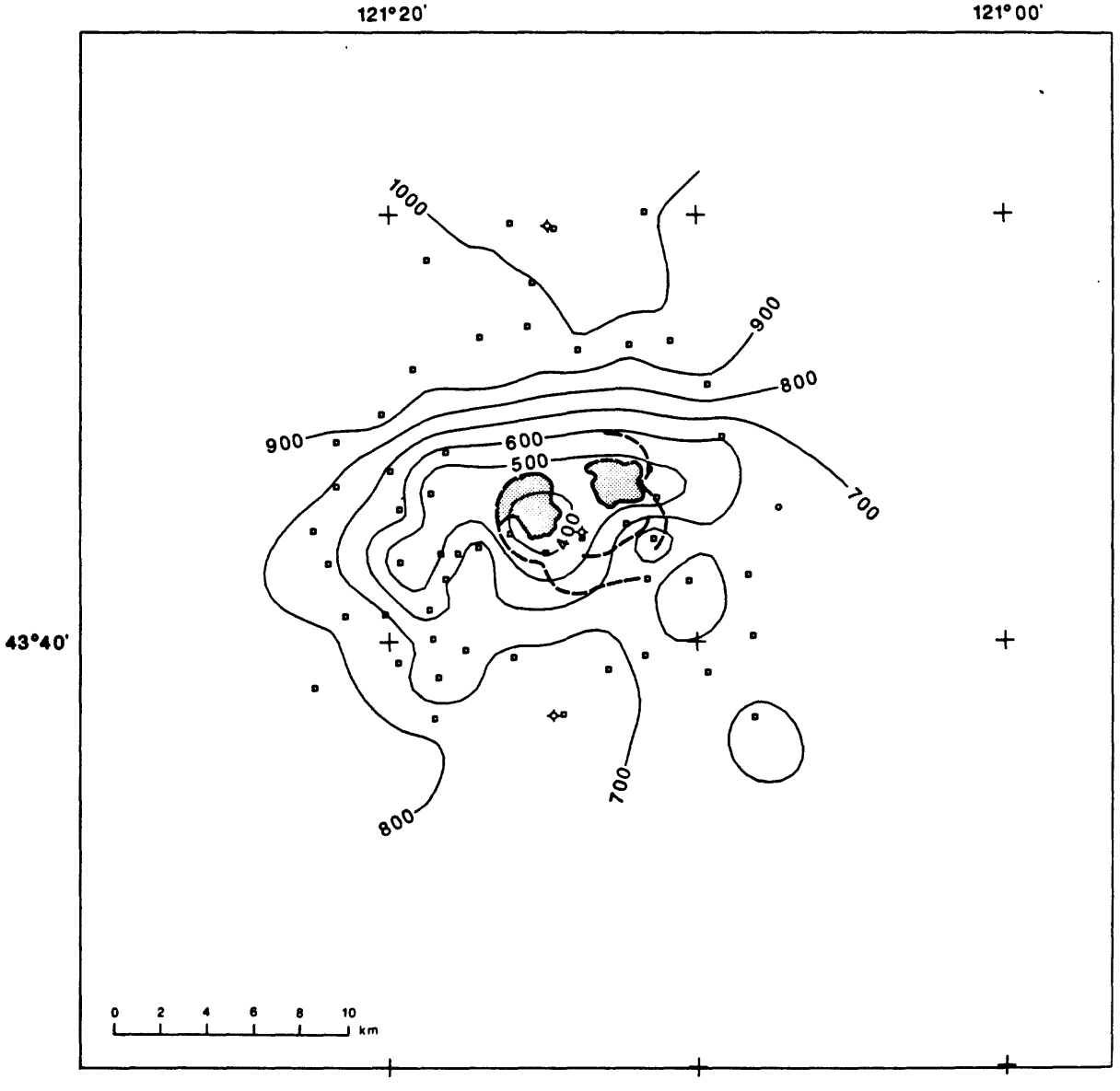
121°20'
121°00'
43°40'
1000
900
800
900
600
500
400
700
700
800
0 2 4 6 8 10
km

10

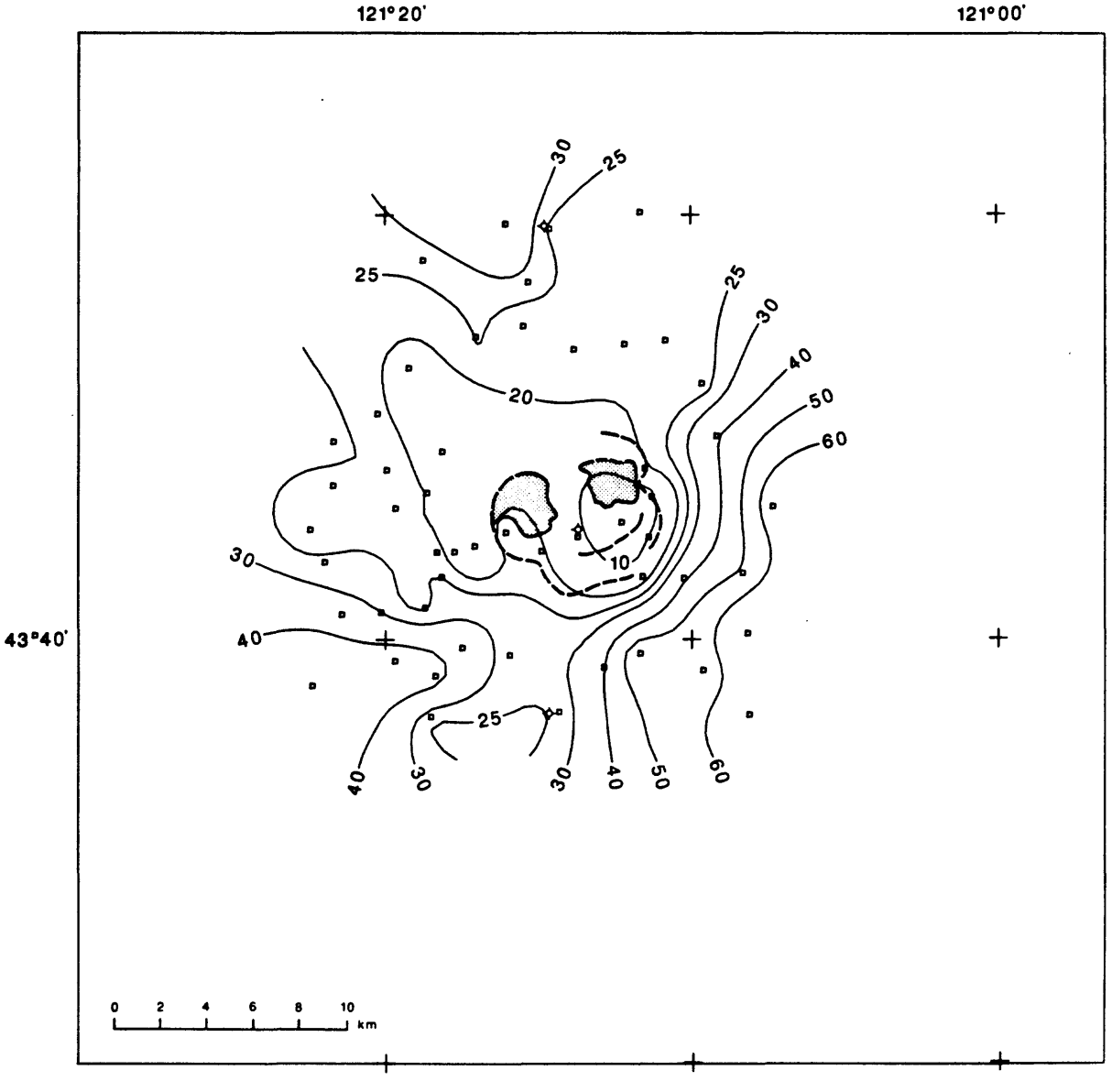
121°20'
121°00'
43°40'
30
25
25
20
25
30
40
50
60
10
30
40
25
40
30
30
40
50
60
0 2 4 6 8 10
km

11

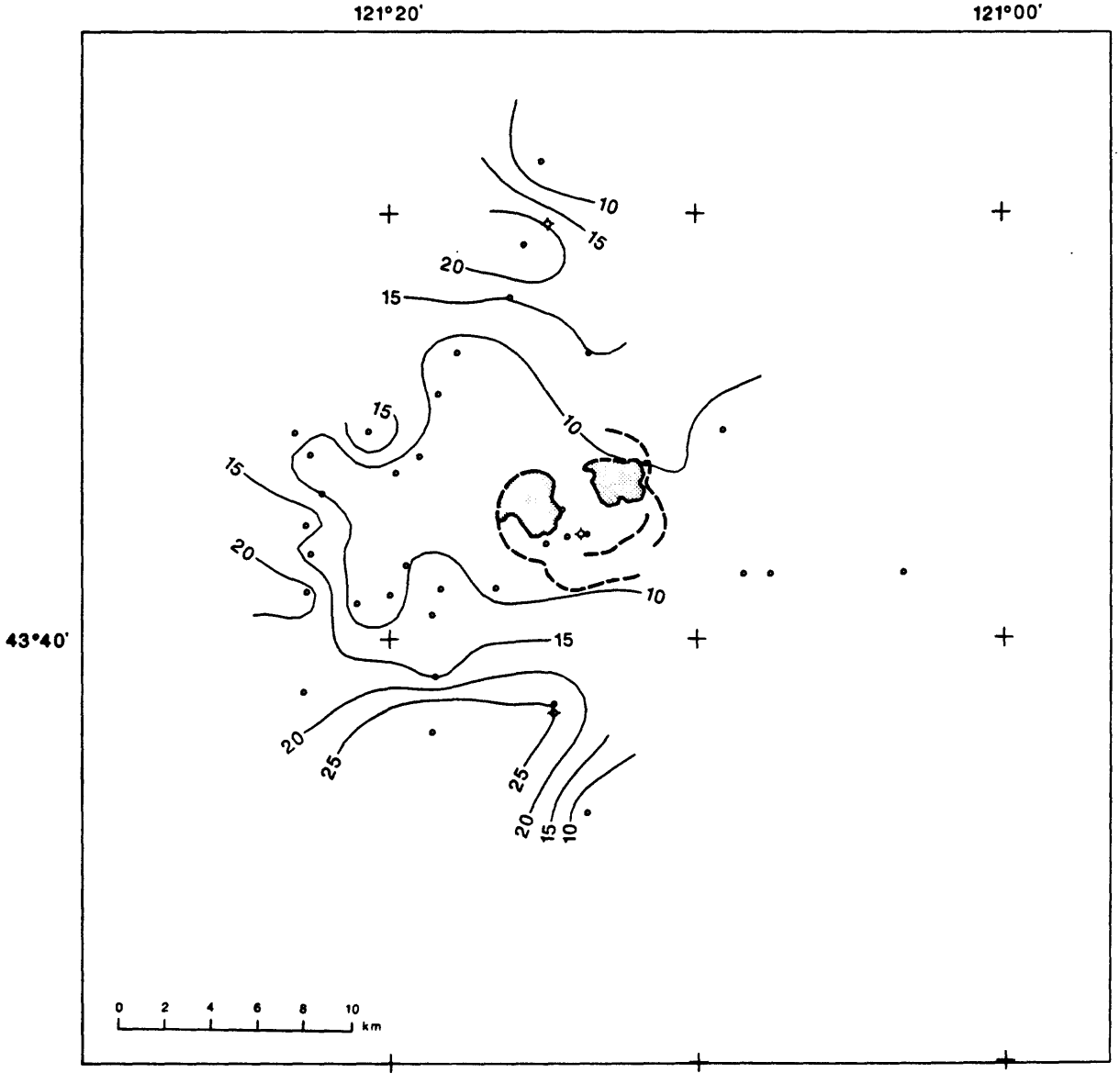
121°20'
121°00'
43°40'
10
15
20
15
15
10
15
20
10
15
20
25
25
20
15
10
0 2 4 6 8 10
km

12

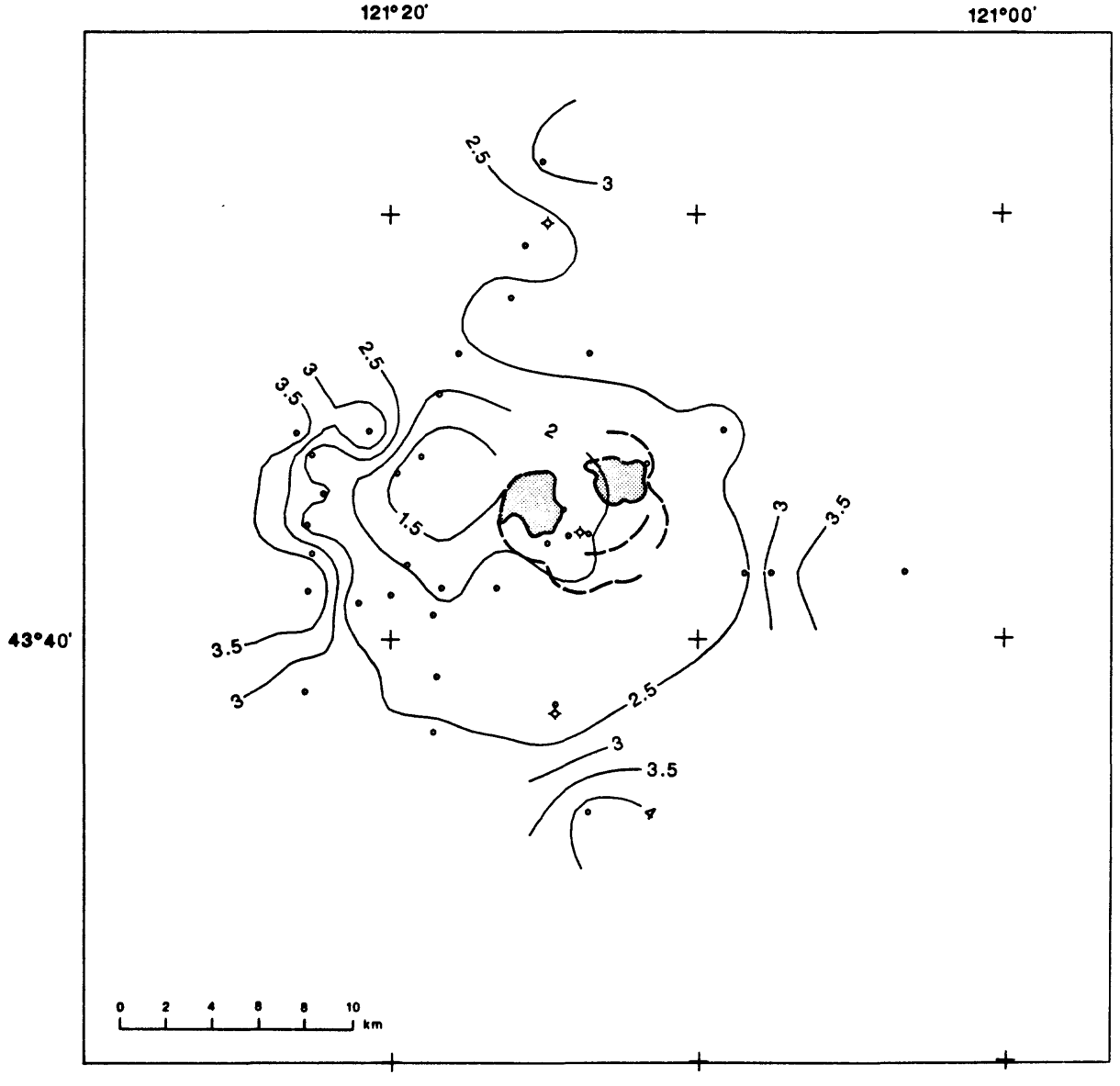
121°20'
121°00'
43°40'
2.5
3
3.5
2
1.5
0 2 4 6 8 10
km

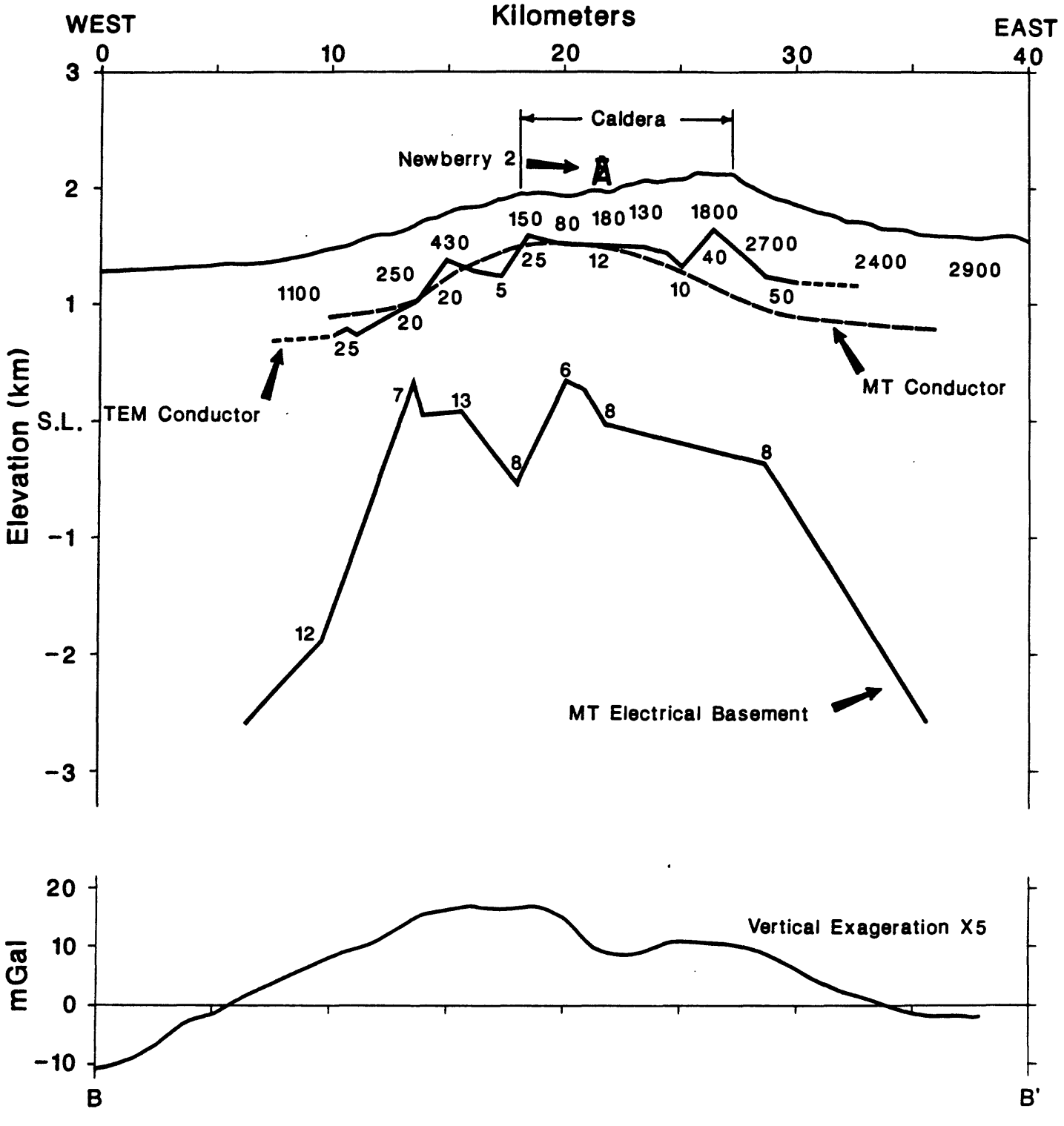
WEST
Kilometers
EAST
0
10
20
30
40
3
2
1
S.L.
-1
-2
-3
Elevation (km)
Caldera
Newberry 2
A
A'
150
80
180
130
1800
430
2700
250
25
12
40
2400
2900
1100
20
5
10
50
20
25
TEM Conductor
MT Conductor
7
13
6
8
8
8
12
MT Electrical Basement
20
10
0
-10
mGal
Vertical Exageration X5
B
B'

USGS Newberry 2, Newberry Volcano

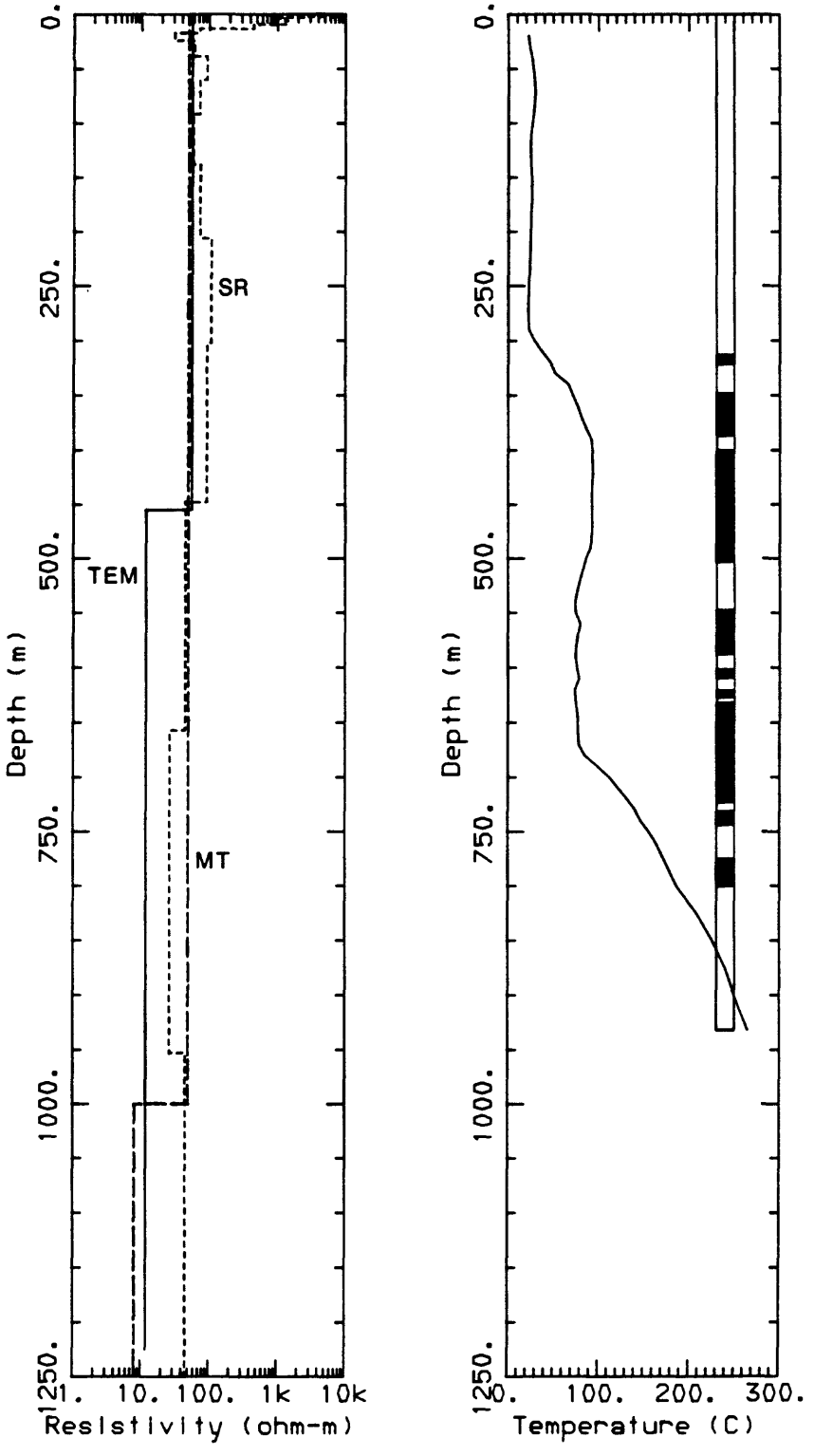

GEO-Operator N-1, Newberry Volcano

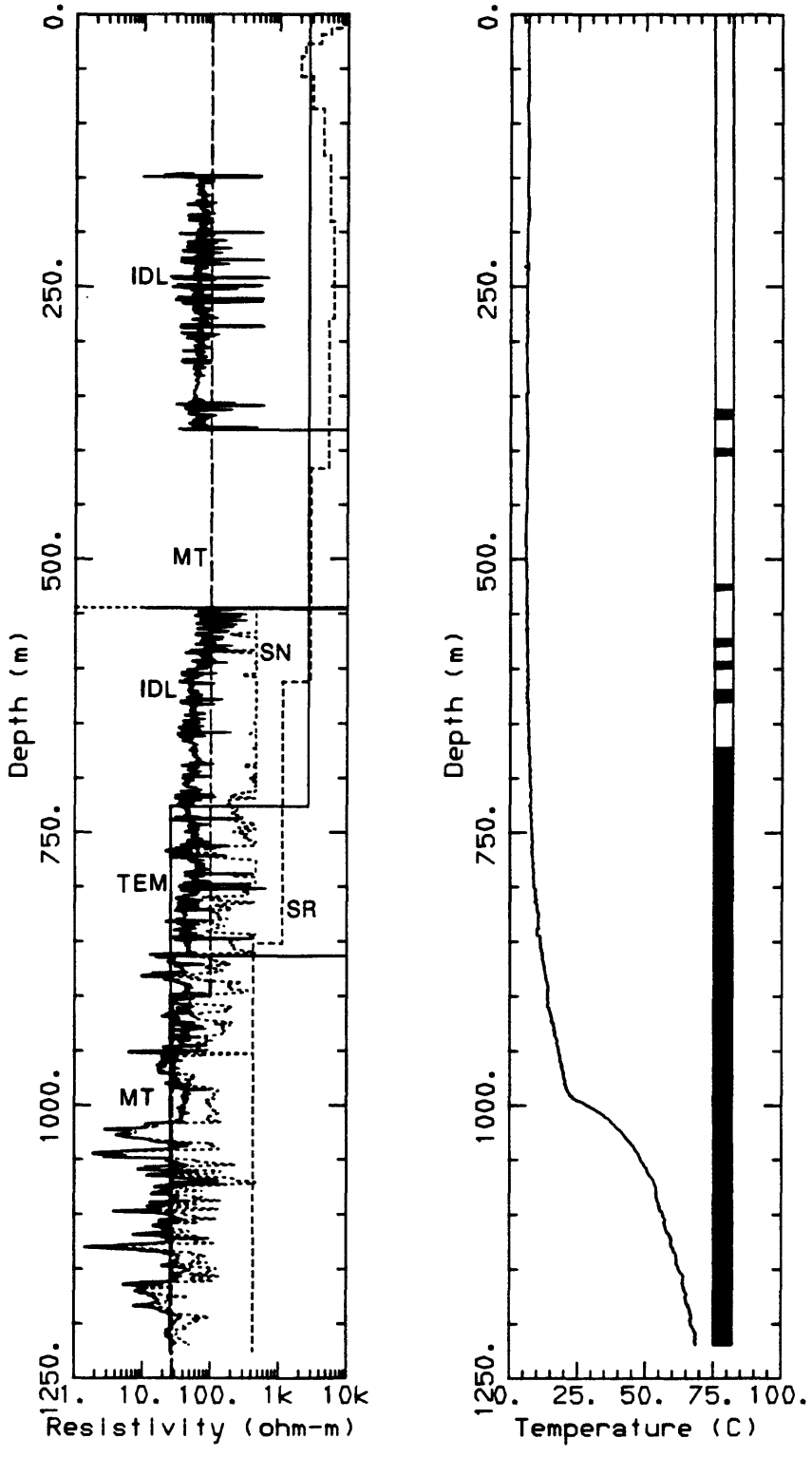

GEO-Operator N-3, Newberry Volcano

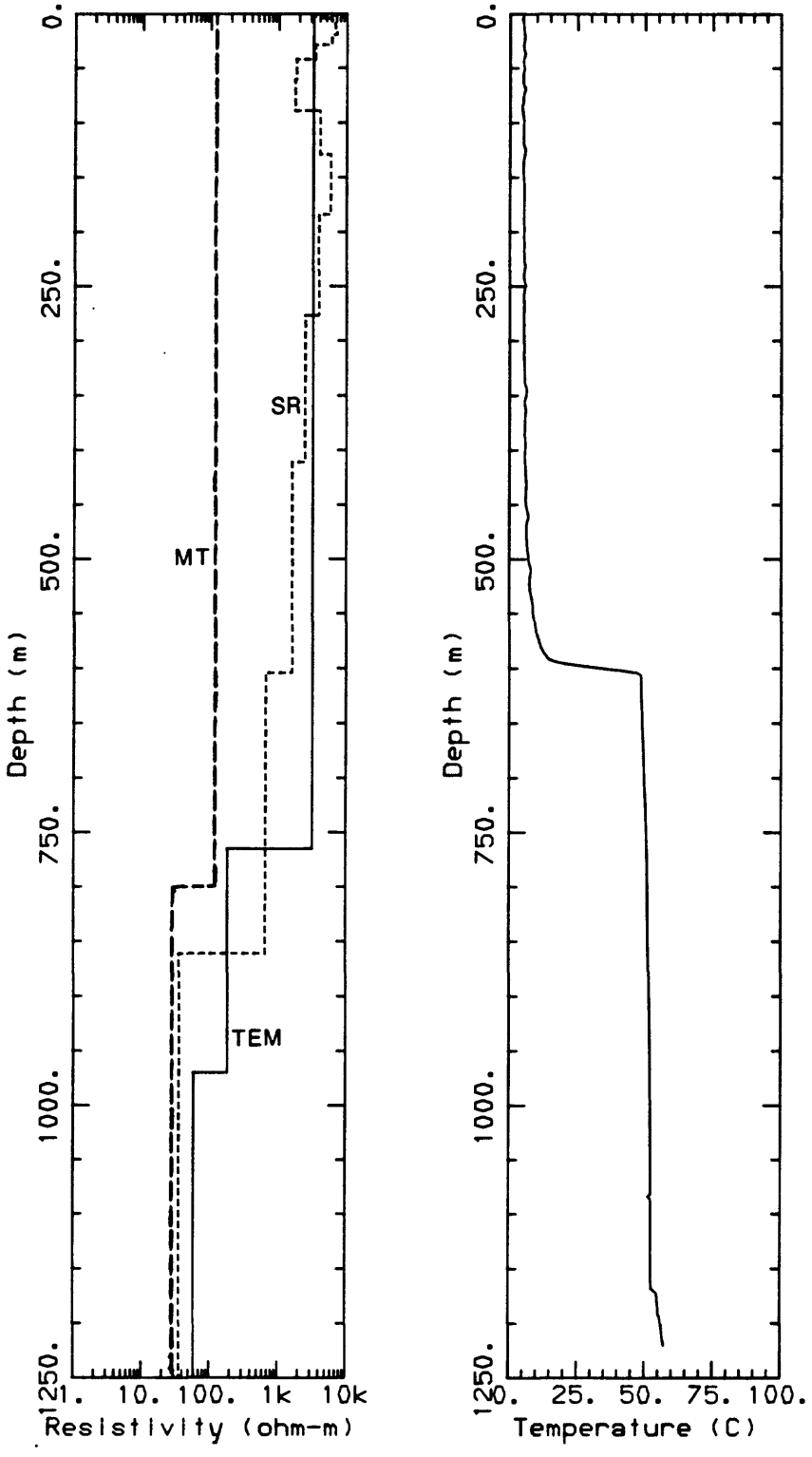

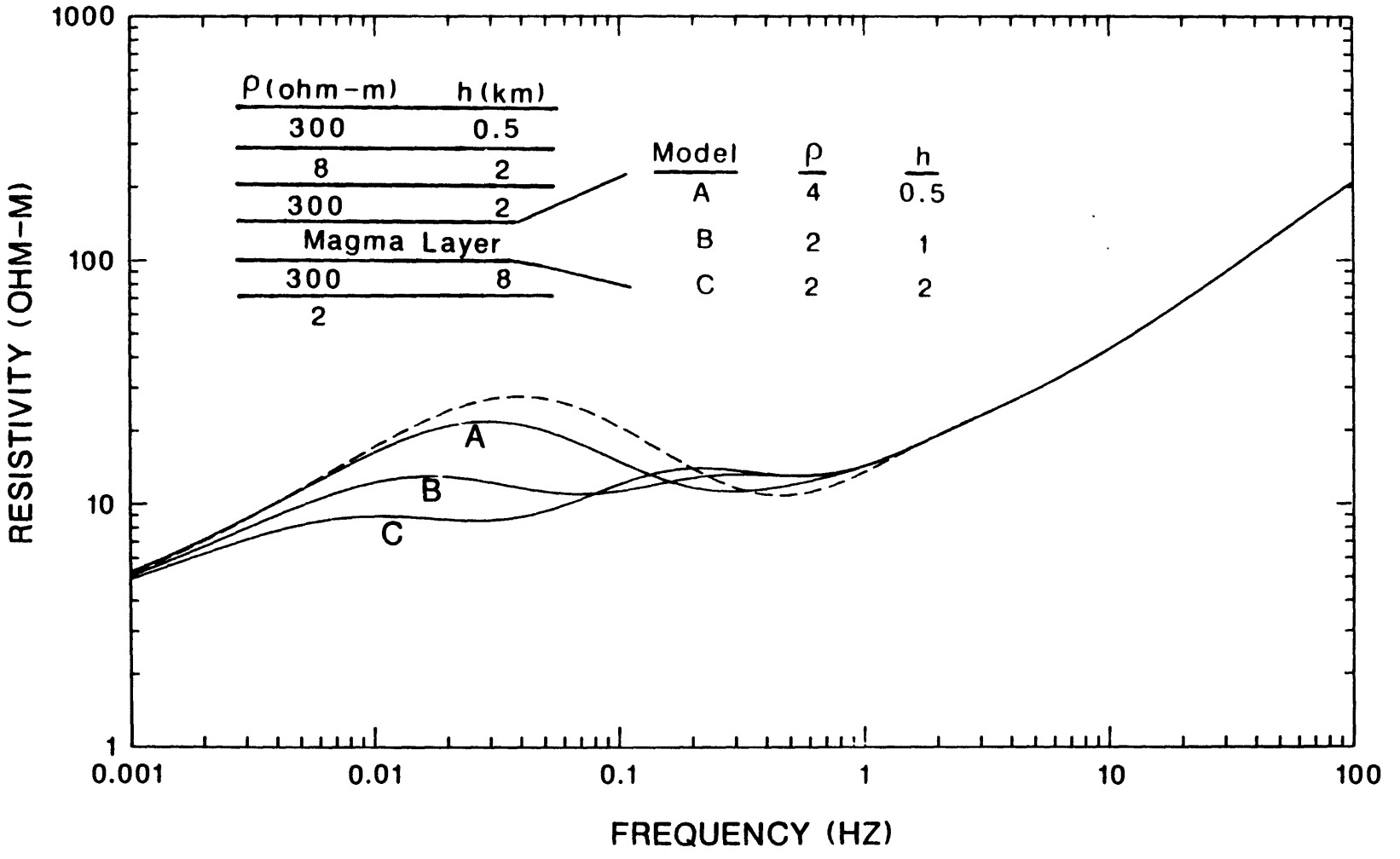
1000
100
10
1
RESISTIVITY (OHM-M)
0.001
0.01
0.1
1
10
100
FREQUENCY (HZ)
ρ(ohm-m) h(km)
300 0.5
8 2
300 2
Magma Layer
300 8
2
Model ρ h
A 4 0.5
B 2 1
C 2 2
A
B
C

45